Fuel Optimal Rendezvous Including a Radial Constraint.

by

Gopal Vasudevan

Thesis submitted to the Faculty of the

Virginia Polytechnic Institute and State University

in partial fulfillment of the requirements for the degree of

Master of Science

in

Aerospace & Ocean Engineering

APPROVED:

Dr.F.H. Lutze, Chairman

Dr.H.J. Kelley

Dr.E.M. Cliff

August, 1986

Blacksburg, Virginia

Fuel Optimal Rendezvous Including a Radial Constraint.

by

Gopal Vasudevan

Dr.F.H. Lutze, Chairman

Aerospace & Ocean Engineering

(ABSTRACT)

Fuel-optimal rendezvous in orbit is examined using thrust-impulses and coasting arcs. Necessary conditions for the optimality of fuel-optimal rendezvous with and without radial constraints are derived. These conditions are then used to verify the optimality of trajectories obtained from a parameter-optimization technique.

For rendezvous problems with radial constraint, locally optimal trajectories include constrained arcs or touch-point arcs. Numerical procedures to compute the costates and the jumps in the costates at the touch point and at the entry point to the constraint arc are provided. Locally optimal solutions for non-optimal trajectories with a minimum radius-constraint are obtained using criteria due to Lion and Handelsmann.

Numerical solutions show that multiple-impulse trajectories almost always result in a lower cost function than the corresponding two impulse trajectories. It is also observed that trajectories comprised of only touch-point arcs can often be improved by using an additional impulse.

Acknowledgements

The author wishes to express his deep appreciation to his advisor, Dr. Frederick H. Lutze without whose invaluable guidance and assistance this study may not have been possible.

Thanks are also due to Dr. Eugene M. Cliff, Dr. Henry J. Kelley and Dr. John A. Burns for their helpful comments and suggestions towards the fulfillment of this endeavor.

He also wishes to thank his fellow graduate students for their help and assistance.

Table of Contents

1.0 Introduction. **1**

2.0 Unconstrained Problem **6**

2.1 Lawden's Problem 6

2.2 Equations of Motion 7

2.3 Necessary Conditions for Optimality 9

2.3.1 Coasting arc 12

2.3.2 Intermediate-Thrust Arc 12

2.3.3 Impulse Thrusts 14

2.3.4 Maximum-Thrust Arc 16

2.4 Summary 17

3.0 Numerical Solutions of Unconstrained Problem **18**

3.1 Introduction 18

3.2 Computational Procedure 21

3.3 Examples 27

3.4 Discussion 30

4.0 Constrained Problem **35**

4.1 Introduction 35

4.2 Necessary Conditions 36

4.3 Computational Procedure 41

4.3.1 Constraint Arc 42

4.3.2 Touch Point Arcs 44

4.4 Examples and Discussions 48

5.0 Summary **52**

References **54**

Figures **57**

Appendix A. Solutions to the Costate Equations. **74**

Appendix B. Notes on Parameter Optimization **81**

Vita **84**

List of Illustrations

Figure 1. Geometry of Orbit. 58

Figure 2. Variation of the Characteristic Velocity with total time for Unconstrained Circle-to-Circle Rendezvous Problem. 59

Figure 3. Rendezvous Trajectory between two circles of radius ratio = 1.2 for total time to rendezvous = 7.437 TU 60

Figure 4. Rendezvous Trajectory between two circles of radius ratio = 1.2 for total time to rendezvous = 10.41 TU 61

Figure 5. Two-Impulse Time Free Rendezvous Trajectory between two Ellipses of different eccentricity. 62

Figure 6. Two-Impulse near rectilinear Time Free Rendezvous Trajectory between two Ellipses of different eccentricity. 63

Figure 7. Time history of the Primer-Vector Magnitude of the trajectory corresponding to figure.5. 64

Figure 8. Time history of the Primer-Vector Magnitude of the trajectory corresponding to figure.6. 65

Figure 9. Three-Impulse Time Free Rendezvous Trajectory between two Ellipses of different eccentricity. 66

Figure 10. Time history of the Primer-Vector Magnitude of the trajectory corresponding to figure.9. 67
Figure 11. Variation of the Characteristic Velocity with total time for unconstrained ellipse-to-ellipse rendezvous problem. 68
Figure 12. Rendezvous Trajectory between two circles including a Constraint Arc. 69
Figure 13. Rendezvous Trajectory between two circles including a Touch-Point. 70
Figure 14. Variation of the Characteristic Velocity with total time for Circle-to-Circle Rendezvous including Minimum Radius. 71
Figure 15. Variation of the Characteristic Velocity with Constraint Radius. 72
Figure 16. Variation of the Characteristic Velocity with Constraint Radius. 73

List of Symbols

a .....semi-major axis

c.....jet exhaust velocity

e.....eccentricity

$\hat{e}$ .....unit vector in the thrust direction

E.....eccentric anomaly

h .....angular momentum

H .....Hamiltonian

I.....identity matrix

J.....cost function

l_r .....direction cosine of the thrust vector in the radial direction

l_θ.....direction cosine of the thrust vector in the tangential direction

m .....mass of the rendezvous vehicle

n .....number of impulses

$\bar{p}$ .....primer vector

p .....norm of the primer vector

$\bar{r}$ .....position vector

r.....norm of the position vector

r_a.....apogee radius

r_p.....perigee radius

R_0 .....minimum radius

S .....state constraint

t.....time of flight

T.....time period of an orbit

T_H.....Hohmann time

T_ψ.....phasing time required for a Hohmann transfer

T_s.....synodic period

v .....radial velocity

V .....total velocity

ΔV.....characteristic velocity

ΔV_r.....change in radial velocity

ΔV_θ.....change in tangential velocity

ΔV_{tot}.....total change in velocity

W .....weighting factor

Greek symbols

β .....thrust magnitude

γ .....Lagrange multiplier associated with the state constraint

$\delta_{i,j}$.....kronecker delta

η_i .....angle of coast on the i^{th} subarc

θ .....true anomaly

λ-.....vector of costate variables

μ .....Lagrange multiplier

μ_0 , μ_1.....jumps in costates

σ.....switching function

Φ , Ψ .....transition matrices

$\varphi_{i,j}$ .....elements of the transition matrix

ψ.....relative phase of the target with respect to the rendezvous vehicle

ω.....angular rate

Superscripts

T.....transpose

-1.....inverse

$+$ .....after an event

$-$ .....before an event

$'$ .....derivative with respect to the true anomaly

Subscripts

0 .....initial state

f.....final state

RV.....rendezvous vehicle

T.....target

en .....entry point to a constraint arc

ex.....exit point to a constraint arc

1.0 Introduction.

Minimum-fuel transfer between orbits in an inverse-square gravitational field is one of the oldest problems in space-flight optimization. One version of this problem assumes a finite number of impulses and coasting arcs to accomplish some space-flight maneuver such as intercept, rendezvous or simply an orbital transfer. Interest in this version stems from the fact that impulses provide a convenient approximation to short thrusting periods. This facilitates modelling the fuel optimization problem for some space-flight maneuvers for solution via a parameter optimization method.

For a given final time, a rendezvous with a non-maneuvering target or an orbital transfer can be accomplished using two impulses. In fact for a circle-to-circle orbit transfer, for a large enough time and for a ratio of the final radius to initial radius less than 11.94, a particular type of two impulse transfer, known after its discoverer and called a Hohmann transfer is the most fuel efficient [Edelbaum,1967], [Marec, 1979]. However, when the total time is limited

or when the radius ratio becomes greater than 11.94, more impulses may be necessary for optimality. Indeed Hoelker and Silber [1961] found bi-elliptic transfers to be fuel-optimal for transfers between orbits with radius ratios in excess of 11.94. A good insight to the general nature of fuel optimal transfers and rendezvous problems can be found in the survey papers by Edelbaum [1967] and by Gobetz and Doll [1969].

In applications work total maneuvering time is often limited and yet fuel efficient transfers must be achieved. It would be of interest from the standpoint of parameter optimization, whether or not a fuel-optimal maneuver can be accomplished using a finite number of impulses. It has been shown by Neustadt [1964] and by Potter and Stern [1965] that for a linearized problem, a minimum-fuel transfer between neighboring orbits can always be done with a number of impulses at most equal to the the number of terminally specified state variables. Thus, for a coplanar rendezvous problem with a nonmaneuvering target using a linear analysis at most four impulses are required and for a non-coplanar problem at most six. Unfortunately, not much can be said on the upper limit on the number of impulses for the nonlinear problem, and less if state constraints are considered.

A comprehensive study of spaceflight optimization is due to Lawden [1959], [1962], [1963] who provided a set of necessary conditions for fuel-optimal space maneuvers. Reference [1963] provides the necessary conditions for optimality in terms of " primer vector " for the problem of a rocket with a constant jet exhaust velocity and variable thrust magnitude and direction in a general gravitational

field. The primer vector is defined as the vector of the costate variables corresponding to the velocity components. Lion and Handelsmann [1968] later extended the primer-vector theory to nonoptimal trajectories to indicate how time-fixed trajectories could be improved by introducing either additional impulses or by adding initial or final coasts. Using this theory, Prussing [1969], [1970] provided a method of solution for the linearized version of multi-impulse fixed time circle-to-circle rendezvous problem. He linearized the equations of motion about a reference circular orbit, in the vicinity of the terminal orbits, and then solved the boundary-value problem analytically. Glandorf [1969] investigated the nonlinear problem for both bounded and impulsive thrusting and included the radial constraint in his analysis. Numerical results for two-impulse fixed-time rendezvous and for one- and two-impulse fixed-time intercept problems were also presented. Chiu [1984], [1986] analyzed the nonlinear time-fixed multi-impulse rendezvous problem, and outlined a procedure for its solution. He also considered the out-of-plane circle-to-circle rendezvous.

Neustadt [1966] showed that any minimum-fuel solution to Lawden's problem can be approximated arbitrarily closely with a finite number of impulses and coasting arcs. An impulse represents an instantaneous change in velocity. Assuming that the trajectory is comprised solely of impulses and coasting arcs, the fuel-optimal rendezvous problem reduces to the selection of an optimal number of impulses in terms of their points of application along the trajectory and their magnitudes and directions. This formulation of the fuel-optimal

rendezvous problem makes it particularly suited to solution using parameter optimization techniques.

One way to obtain trajectories using parameter optimization is to fix *a priori* the number of impulses. This leads to solving a sequence of Kepler and Lambert type problems between the impulses, where the subarcs connecting the impulses are found by minimizing the sum of the absolute changes in total velocity in going from one subarc to the other. Using this idea, Lutze *etal* provided a procedure to obtain fuel-optimal trajectories for a fixed number of impulses between orbits of arbitrary eccentricity. However, the solution obtained from the parameter optimization technique is merely the minimum ΔV solution for a given or for a fewer number of impulses.

The objective of the present study is to apply the criterion developed by Lion and Handelsmann [1968] to indicate possible need for an additional impulse in solving a general-orbital rendezvous problem with a limited number of impulses. A solution to the time-limited rendezvous problem with a specified number of impulses is obtained using the Kelley-Speyer variable-metric gradient-projection algorithm [Lefton and Kelley, 1978]. Changes in the velocity components at each impulse and the angles of coast on each subarc of the rendezvous vehicle trajectory and the angle of coast of the target are used as variables in the parameter-optimization procedure. The performance index (cost function) considered is the sum of the absolute values of the changes in velocity at each impulse. At the conclusion of the parametric optimization, if the angle of coast on a free-fall subarc is found to be equal to a prescribed bound, this is taken to

indicate coalesence of impulses. The solution obtained may then be used to compute the time history of the primer vector to check for optimality. If the magnitude of the primer vector becomes greater than unity at any point on the trajectory, an additional impulse should be considered. The parametric nature of the method of solution automatically allows for an optimal initial coast. Since the problem obtains a time-limited optimal trajectory, terminal coast is also accounted for.

In practical problems, all maneuvers must be performed in a manner such that the attracting body is not penetrated; trajectories must not violate a minimum radius constraint. To this end, the fuel-optimal problem may be reformulated incorporating a radius inequality constraint. The necessary conditions for optimality derived from the Minimum Principle may then be used to verify the trajectories obtained from parameter optimization with constraint, in a manner similar to that used for the unconstrained problem. Numerical procedures are provided to obtain the costates on touch-point arcs and constraint arcs.

2.0 Unconstrained Problem

2.1 Lawden's Problem

Pioneering work in the area of spaceflight path optimization is due to Lawden, who considered transfers in a general gravitational field. Because of his efforts the following has come to be known as Lawden's problem [Edelbaum,1967]: Determine a minimum-fuel transfer between orbits in an inverse-square gravitational field for a variable-thrust rocket having constant exhaust velocity and an unbounded thrust magnitude.

For a rocket moving under only its own thrust

$$\dot{V} = -\frac{c}{m}\frac{dm}{dt} \qquad [2.1.1]$$

where c = jet exhaust velocity

V = total velocity.

If the exhaust velocity c is maintained constant, the above equation can be integrated to yield over $[t_0, t_f]$

$$V_f - V_0 = c \ln \frac{m_0}{m_f} \qquad [2.1.2]$$

The magnitude of the velocity increment caused by the expenditure of fuel which decreases the mass of the rocket from m_0 to m_f is given by

$$\Delta V = c \ln \frac{m_0}{m_f} \qquad [2.1.3]$$

ΔV is called the characteristic velocity for the maneuver.

2.2 *Equations of Motion*

In the presence of a central gravitational field, satellite motions lie in a plane. Therefore for maneuvers with a target lying in the same plane as the interceptor, two spatial coordinates are sufficient to describe the position at any time. Since motion in the absence of thrust maybe described by conic sections, it is natural to use polar coordinates. Choosing (r, θ) to be the coordinates, the equations of motion of a body moving in an inverse square gravitational field under thrust

can be written by a straightforward application of Hamilton's equations. Normalizing the variables with respect to the earth radius and choosing the time unit to be such that the gravitational constant is unity, the equations of motion can be written as follows:

$$\dot{r} = v \qquad [2.2.1]$$

$$\dot{\theta} = \frac{h}{r^2} \qquad [2.2.2]$$

$$\dot{v} = \frac{h^2}{r^3} - \frac{1}{r^2} + \frac{c\,\beta\,l_r}{m} \qquad [2.2.3]$$

$$\dot{h} = \frac{r\,c\,\beta\,l_\theta}{m} \qquad [2.2.4]$$

$$\dot{m} = -\beta \qquad [2.2.5]$$

subject to constraints on the control variables as

$$l_r^2 + l_\theta^2 - 1 = 0 \qquad [2.2.6]$$

$$-\beta \leq 0 \qquad [2.2.7]$$

$$\beta - \beta_m \leq 0 \qquad [2.2.8]$$

where β is the mass flow rate and l_r and l_θ are the direction cosines of the thrust vector in the radial and transverse directions respectively.

2.3 *Necessary Conditions for Optimality*

The problem at hand is then to find a trajectory for a rendezvous with a nonmaneuvering target for a minimum of the characteristic velocity, or equivalently, a minimum of the initial mass given the final mass, or maximum of the final mass given the initial mass. This leads to

$$J = c \ln \frac{m_0}{m_f} \qquad [2.3.1]$$

as the performance index. To obtain an optimal trajectory the Hamiltonian is formed as

$$H = \lambda_r v + \lambda_\theta \frac{h}{r^2} + \lambda_v \left(\frac{h^2}{r^3} - \frac{1}{r^2} + \frac{c\beta l_r}{m}\right) + \frac{\lambda_h r c \beta l_\theta}{m} - \lambda_m \beta + \mu(l_r^2 + l_\theta^2 - 1) \qquad [2.3.2]$$

where λ_r , λ_θ , λ_v , λ_h and λ_m are the adjoint or the costate variables.

The first order necessary conditions for a minimum include the Euler-Lagrange equations

$$\dot{\lambda}_r = 2\lambda_\theta \frac{h}{r^3} + \lambda_v \left(\frac{3h^2}{r^4} - \frac{2}{r^3}\right) - \frac{\lambda_h c \beta l_\theta}{m} \qquad [2.3.3]$$

$$\dot{\lambda}_\theta = 0 \qquad [2.3.4]$$

$$\dot{\lambda}_v = -\lambda_r \qquad [2.3.5]$$

$$\dot{\lambda}_h = \frac{-\lambda_\theta}{r^2} - 2\lambda_v \frac{h}{r^3} \qquad [2.3.6]$$

$$\dot{\lambda}_m = (\lambda_v l_r + \lambda_h r l_\theta) \frac{c\beta}{m^2} \qquad [2.3.7]$$

From the Minimum Principle the control variables l_r , l_θ and β are chosen so as to satisfy :

$$\lambda_v \frac{c\beta}{m} + 2\mu l_r = 0 \qquad [2.3.8]$$

$$r\lambda_h \frac{c\beta}{m} + 2\mu l_\theta = 0 \qquad [2.3.9]$$

and the mass flow rate β is such that it minimizes the Hamitonian H. Setting

$$M(\underline{\lambda}, \underline{x}) \equiv \min_{\beta} \{[(\lambda_v l_r + r\lambda_h l_\theta)\frac{c}{m} - \lambda_m]\beta\} + \lambda_r v + \lambda_\theta \frac{h}{r^2} + \lambda_v (\frac{h^2}{r^3} - \frac{1}{r^2}) \qquad [2.3.10]$$

$M(\underline{\lambda}, \underline{x})$ is constant over the entire trajectory.

Define vectors

$$\bar{p} \equiv \{\lambda_v , r\lambda_h\} \qquad [2.3.11]$$

$$\hat{e} \equiv \{l_r , l_\theta\} \qquad [2.3.12]$$

then equation [2.3.10] can be rewritten as

$$M(\underline{\lambda}, \underline{x}) = \min_{\beta} \{ [(\bar{p} \cdot \hat{e}) \frac{c}{m} - \lambda_m] \beta \} + \lambda_r v + \lambda_\theta \frac{h}{r^2} + \lambda_v (\frac{h^2}{r^3} - \frac{1}{r^2}) \quad [2.3.13]$$

Thus it can be seen that for any non-zero mass flow rate β the minimum value for the above expression is attained when $\bar{p} \cdot \hat{e} = -p$, where p is the norm of $\bar{p}$. Using this in equations (2.3.8) and (2.3.9), the primer-vector components on a thrusting arc are given by:

$$\lambda_v = -l_r p \quad [2.3.14]$$

$$r \lambda_h = -l_\theta p \quad [2.3.15]$$

These imply that the thrust vector is opposite in direction to the primer vector. From [2.3.13] a switching function can be defined as:

$$\sigma = -\frac{c p}{m} - \lambda_m \quad [2.3.16]$$

By examining equation [2.3.16] it is seen that the switching function σ takes on a negative value on the maximum thrust arc, zero on the intermediate thrust arc and is positive on the coasting arc. For a better understanding of the problem it would be worthwhile to examine each of these cases separately.

2.3.1 Coasting arc

An arc over which the thrust magnitude is zero is called a coasting arc. On this arc λ_m is a constant and from the definition of the switching function it is seen that

$$-\frac{m\lambda_m}{c} \geq p \qquad [2.3.17]$$

These arcs are conic sections, defined by the initial and final conditions and the traversing time over each subarc. Along these arcs closed form solutions for the costate equations exist in the terms of simple functions which are given in Appendix A.

2.3.2 Intermediate-Thrust Arc

On an intermediate-thrust arc the switching function becomes identically zero. Consequently, the thrust magnitude can not be evaluated directly from the Minimum Principle. Therefore, successive time derivatives of the switching function σ are obtained and set to zero. Since the thrust magnitude β is a second-order singular control, it can be determined from the fourth time derivative of the switching function.

By setting the switching function to zero

$$\lambda_m = - \frac{c\,p}{m} \qquad [2.3.18]$$

Substituting this into equation [2.3.7] and making a transformation to a derivative with respect to mass using [2.2.5], yields on straightforward integration

$$\lambda_m = \frac{k}{m} \qquad [2.3.19]$$

where k is some constant. Therefore, by comparing (2.3.18) and (2.3.19), it is apparent that the primer vector has a constant magnitude on an intermediate thrust arc. The Transversality condition for $\lambda_m|_{t=t_f}$ is given as :

$$\begin{aligned} \lambda_m|_{t=t_f} &= \frac{\partial J}{\partial m_f} \\ &= - \frac{c}{m_f} \end{aligned} \qquad [2.3.20]$$

Thus for an intermediate thrust arc terminating at $t = t_f$

$$\lambda_m|_{t=t_f} = \frac{k}{m_f} = - \frac{c}{m_f} \qquad [2.3.21]$$

Or $k = - c$ giving thus that $p = 1$ on a terminal intermediate thrust arc.

2.3.3 Impulse Thrusts

In the limit as β_m tends to infinity, the thrust capability becomes unbounded. Therefore any thrust phase over a very short time duration can be approximated by an impulsive thrust. In this context, an impulse represents a change in the velocity of the vehicle without affecting its position. This is in contrast to a *generalized impulse,* which allows a prescribed discontinuity in the position vector normal to the velocity change [Robbins,1966].

In order to determine the changes in the states and costates across these impulsive arcs, the state and costate equations can be rewritten with mass as the independent variable instead of time using the transformation

$$-\beta\frac{d(.)}{dm} = \frac{d(.)}{dt}. \qquad [2.3.22]$$

In the limit as the mass flow rate and hence thrust magnitude tend to infinity, it is observed that across an impulse, $r, \theta, \lambda_\theta, \lambda_v$ and λ_h do not change, whereas v, h, m, λ_r and λ_m experience a jump given by:

$$\Delta v = c\, l_r \ln\frac{m^-}{m^+} \qquad [2.3.23]$$

$$\Delta h = r\, c\, l_\theta \ln\frac{m^-}{m^+} \qquad [2.3.24]$$

$$\Delta m = m^+ - m^- \qquad [2.3.25]$$

$$\Delta\lambda_r = -c\,\lambda_h\,l_0\,\ln\frac{m^-}{m^+} \qquad [2.3.26]$$

$$\Delta\lambda_m = -c\,p\,(\frac{1}{m^+} - \frac{1}{m^-}) \qquad [2.3.27]$$

Since impulses are simply intermediate thrust arcs over an infinitesimally small time duration, the primer vector has a unit magnitude at a terminal impulse. It can be shown that the primer vector has a unit magnitude at an impulse on a trajectory comprising of only impulses and coasting arcs with an impulse at either end of the transfer trajectory.

Consider a trajectory composed of only coasting arcs and impulses with an impulse at the end of the final coasting arc. From equation [2.3.21] the value of the costate λ_m is known at end of terminal impulse. Since the primer vector has a unit magnitude at the terminal impulse, the λ_m at the start of the terminal impulse can be computed from equation [2.3.27]. Now, on the coasting arc λ_m is a constant. Hence, λ_m is known at the end of the penultimate impulse. Or

$$(\lambda_m)_{n-1} = -\frac{c}{m_f^-} \qquad [2.3.28]$$

where n is the number of impulses. Therefore using [2.3.27], it is seen that $k = -c$. Using the definition of the switching function and equation [2.3.28], it can be shown that

$$p = 1. \qquad [2.3.29]$$

at the penultimate impulse.

Following the same sequence of arguments for each impulse, it is observed that at the impulse, the primer vector has a unit magnitude. Now λ_m is a constant on the coasting arc and is given by $\lambda_m = -\frac{c\,p}{m}$. Therefore from equation [2.3.16] it is apparent that the primer vector must have a magnitude less than or equal to unity on the coasting arc. Considering the differential cost between two neighboring trajectories at an intermediate impulse it has been shown by Lion and Handelsmann [1968] that:

1. Hamiltonian is a constant over the entire optimal trajectory.
2. $\dot{p} = 0$ at an intermediate impulse.

This is evident from the fact that the Hamiltonian does not explicitly depend on time and since the point of application of an impulse is not fixed in time. The second conclusion can be shown by examining the difference in the Hamiltonian across an impulse.

2.3.4 Maximum-Thrust Arc

On this arc the thrust magnitude or equivalently the mass flow rate assumes its maximum value. From the definition of the switching function it is observed that

$$-\frac{m\lambda_m}{c} \leq p \qquad [2.3.30]$$

As in the case of the intermediate thrust arc, the thrust is opposite in direction to the primer vector. No closed-form solutions to this case are known to exist, and numerical methods must be resorted to.

This study concerns itself with the preceding two cases and hence the latter case is not examined in detail.

2.4 Summary

The system of necessary conditions, first developed by Lawden, for an optimal trajectory, in the absence of any radial constraints can now be summarized as follows.

1. The primer vector and its first derivative are continuous everywhere.
2. At an impulse, the thrust vector is opposite in direction to the primer vector.
3. The magnitude of the primer vector is less than unity everywhere except at the impulses where it is unity.
4. At all intermediate impulses the time derivative of the primer vector is zero.

3.0 Numerical Solutions of Unconstrained Problem

3.1 Introduction

A time-fixed rendezvous with a nonmaneuvering target can always be accomplished with two impulses. For a number of problems, two-impulse trajectories such as the Hohmann transfer yield the minimum-fuel trajectories. Often such transfers may not even be defined, say for transfers between elliptic orbits with non-parallel axes. Also, if the time to rendezvous is limited, other trajectories involving multiple impulses and intermediate thrust arcs need to be investigated.

From Minimum Principle, fuel-optimal orbital trajectories are comprised of three types of arcs. These are zero-thrust arcs (also called coasting arcs), maximum-thrust arcs and intermediate-thrust arcs (i.e. arcs with positive thrust magnitude less than the maximum thrust). The intermediate-thrust arcs

represents the singular case of the fuel-optimal transfer problem, as the magnitude of the thrust can not be determined directly from the Minimum Principle. Robbins [1965] has shown that under certain restricted conditions, intermediate thrust arcs yield a minimum over short lengths of arc when both initial and final states lie on the intermediate thrust arc. Such arcs however, cannot have corner junctions with either the maximum-thrust arc, or in the absence of any impulses, with the coasting arc. By allowing impulses in the admissible set of controls, the intermediate-thrust arc may be optimal even for initial and final state conditions not lying on the intermediate-thrust arc, so long as the optimality conditions due to Robbins [1965] is met. However, the singular intermediate-thrust arc solution to the problem can be approximated using a finite number of impulses. This was guaranteed by Neustadt [1966], who showed that any minimum-fuel solution to Lawden's problem, including a singular-arc solution, can be approximated arbitrarily closely with a finite number of impulses and coasting arcs.

Using this result established by Neustadt [1966] that a minimum-fuel transfer can always be accomplished approximately by using only impulses and coasting arcs, a procedure is sought, which would indicate whether or not the trajectory generated for a certain fixed number of impulses is optimal or not and, if the trajectory is found to be non-optimal, whether more impulses will improve it. If additional impulses are needed, some information regarding a possible point of application and direction of the impulse would be useful in generating another candidate trajectory. This may be achieved by examining the primer vector along

the trajectory and forming judgements according to the criteria developed by Lion and Handelsmann [1968], which states:

1. If the primer vector exceeds unity immediately after the initial impulse on a subarc and is less than unity for most of the subarc, then the cost function can be reduced by allowing an initial coasting arc.
2. If the primer vector exceeds unity only immediately before the terminal impulse then, the cost can be reduced by allowing a final coasting arc.
3. If the primer vector exceeds unity in some manner not described by these two cases then, the cost can be reduced probably by applying an additional impulse or an initial or a final coasting arc, or a combination of all three. The additional impulse in this case should be applied at the point where the magnitude of the primer vector attains its maximum value and in a direction opposite to the primer vector direction.

As shown by Neustadt [1966], the optimal trajectory for a minimum-fuel transfer problem can be strictly composed of a finite number of impulses and coasting arcs. This makes the problem particularly suited to a solution by parameter optimization. If n be the number of impulses fixed *a priori,* then the trajectory can be split into a maximum of $(n + 1)$ separate parts.

A convenient way of solving a minimum-fuel problem is to set it up as a parameter-optimization problem and to use one of several available techniques to solve it. However, it should be noted that the " optimal solution " obtained is dependent on the initial guess supplied to the optimization procedure, i.e. for a

specified number of impulses. Ideally it would be desirable to determine if more or fewer impulses are likely to provide less fuel consumption than the original selection without having to investigate each possible solution.

The primer-vector theory presented in the previous chapter can be used to examine the solution obtained for one configuration and to test it to see if more impulses would yield lesser fuel consumption. On the other hand if the true optimal solution fewer number of impulses then the parameter optimization scheme should drive one of the impulses to near zero magnitude.

The remainder of this chapter will briefly describe the procedure for obtaining a solution using a parameter optimization algorithm (the Kelley-Speyer variable-metric gradient-projection algorithm) [ref. Lefton and Kelley, 1978 and Kelley, Lefton and Johnson,1978] and in greater detail the procedure to use the results of the parameter optimization to examine the consequences of the primer-vector theory to determine the requirement for an additional impulse.

3.2 Computational Procedure

With this formulation, a trajectory can be described by a set of velocity increments due to thrusting impulses, ΔV_i, and the position or angle of coast, η_i, which occurs along each subarc. In addition it is necessary to keep track of the passive target by noting its angle of coast, η_T. The object is then to select

the ΔV_i, η_i and η_T in such a manner as to minimize fuel consumption and provide a rendezvous within some specified time.

Mathematically, this can be stated as: Minimize

$$J(\Delta V_i, \eta_i, \eta_T) = \sum_{i=1}^{n} W_i |\Delta V_i| \qquad [3.2.1]$$

where

n = number of impulses

W_i = weighting factor for the i^{th} impulse

η_i = angle of coast on the i^{th} subarc

ΔV_i = change in velocity at the i^{th} impulse

while satisfying the rendezvous constraints:

The position match:

$$\bar{r}_T(t_f) - \bar{r}_{RV}(t_f) = 0 \qquad [3.2.2]$$

The velocity match:

$$\bar{V}_T(t_f) - \bar{V}_{RV}(t_f) = 0 \qquad [3.2.3]$$

The time to rendezvous constraint:

$$t_f \leq T_{\max} \qquad [3.2.4]$$

In the current formulation the radius and velocity vectors are represented in the inertial coordinates in the solution procedure. For a fixed number of impulses, a set of values for the parameters which satisfy the rendezvous constraint is used in the Kelley-Speyer variable-metric gradient-projection algorithm as an initial guess. The tolerances are initially chosen so as to allow faster convergence. The resulting solution is then used as an initial guess for the next level convergence and this process is repeated until the desired level of convergence is attained. However, this approach yields only locally optimal solutions as the resulting trajectory is dependent on the initial guess.

The trajectory generated from the parameter optimization scheme can be used to check the primer vector conditions to see if addtional impulses are required . This involves computation of the constants to generate the transition matrix to obtain the costates for any time. The initial and final values of the primer vector components on any subarc are obtained from the results of the parameter optimization method. Knowing this and the transiton matrix at any time, the costates and hence the primer vector can be obtained for any time.

The procedure adopted is simply to treat each subarc as a two impulse trajectory and force the primer vector to be equal to a unit vector in the direction opposite to the thrust vector. Using the trajectory generated from the parameter optimization code, the directions cosines on each two impulse segment are evaluated. This is done by converting the change in velocity vector from inertial coordinates to perifocal coordinates. The radial and transverse direction cosines of the thrust vector $\hat{e}$ are computed at each impulse by:

$$l_r = \frac{\Delta V_r}{\Delta V_{tot}} \qquad [3.2.5]$$

$$l_\theta = \frac{\Delta V_\theta}{\Delta V_{tot}} \qquad [3.2.6]$$

With the knowledge of the state variables after the initial impulse, one may compute the orbital elements of the trajectory [ref. Bate, Mueller and White, 1971]. Costate variables can now be computed using equations [A.18] to [A.34] given in the Appendix A. Costates corresponding to the velocity vectors give the components of the primer vector as defined by (2.3.11). For an optimal trajectory, at the point of application of an impulse the, primer vector components have a magnitude equal to the negative of the radial and the tangential direction cosines of the thrust vector. Consequently equations (3.2.5, 6) determine λ_v and $r\lambda_h$ at the initial and final point of a two impulse segment.

The costate equations satisfy the Euler-Lagrange equations (2.3.3 - 7), which can be rewritten in matrix notation as:

$$\dot{\underset{\sim}{\lambda}}(t) = -\underline{\mathbf{A}}^{\mathrm{T}}(t)\,\underset{\sim}{\lambda}(t) \qquad [3.2.7]$$

where $\underline{A}$ is the system matrix of the equations of motion linearized about the optimal trajectory. The solution of (3.2.7) can be written as

$$\underset{\sim}{\lambda}(t) = \underline{\Phi}(t, t_0)\underset{\sim}{\lambda}(t_0) \qquad [3.2.8]$$

where $\Phi(t, t_0)$ is called the state transition matrix [ref.Kwakernaak & Sivan, 1972].

To compute the transition matrix at any time, the constants B_i , C_i and D_i (as given in the Appendix A) need to be evaluated. Using equations (A.11) and (A.17) the constants B_i and C_i are found using the property of transition matrix that $\Phi(t_0, t_0)$ = Identity matrix. At time $t = t_0$, $\theta = \theta_0$ (the starting true anomaly for that subarc) and $E = E_0$ (the equivalent eccentric anomaly). The constants are computed successively for each $i = 1, 2, 3, 4$ from

$$\begin{bmatrix} \sin\theta_0 & f(\theta_0) \\ \dfrac{-h\cos\theta_0}{r^2} & -g(\theta_0) \end{bmatrix} \begin{Bmatrix} B_i \\ C_i \end{Bmatrix} = \begin{Bmatrix} \delta_{3,i} + \dfrac{\delta_{2,i} h \cos\theta_0}{e} \\ \delta_{1,i} + \dfrac{\delta_{2,i} h^2 \sin\theta_0}{e r^2} \end{Bmatrix} \qquad [3.2.9]$$

where $\delta_{1,i}$, $\delta_{2,i}$ and $\delta_{3,i}$ are the Kronecker delta. Knowing B_i , C_i and using (A.23) D_i can be computed for each i.

Since the direction cosines of the thrust vector are known at the beginning and the end of a coasting subarc, the primer vector is known at these two points. Therefore, from two of the costate equations

$$\begin{Bmatrix} \lambda_v(t_f) \\ \lambda_h(t_f) \end{Bmatrix} = \left[\begin{array}{cc|cc} \varphi_{3\,1}(t_f) & \varphi_{3\,2}(t_f) & \varphi_{3\,3}(t_f) & \varphi_{3\,4}(t_f) \\ \varphi_{4\,1}(t_f) & \varphi_{4\,2}(t_f) & \varphi_{4\,3}(t_f) & \varphi_{4\,4}(t_f) \end{array}\right] \begin{Bmatrix} \lambda_r(t_0) \\ \lambda_\theta(t_0) \\ \lambda_v(t_0) \\ \lambda_h(t_0) \end{Bmatrix} \qquad [3.2.10]$$

$\lambda_r(t_0)$ and $\lambda_\theta(t_0)$ can be computed as :

$$\begin{Bmatrix} \lambda_r(t_0) \\ \lambda_\theta(t_0) \end{Bmatrix} = \begin{bmatrix} \varphi_{3\,1}(t_f) & \varphi_{3\,2}(t_f) \\ \varphi_{4\,1}(t_f) & \varphi_{4\,2}(t_f) \end{bmatrix}^{-1} \begin{Bmatrix} \lambda_v(t_f) - \varphi_{3\,3}(t_f)\,\lambda_v(t_0) - \varphi_{3\,4}(t_f)\,\lambda_h(t_0) \\ \lambda_h(t_f) - \varphi_{4\,3}(t_f)\,\lambda_v(t_0) - \varphi_{4\,4}(t_f)\,\lambda_h(t_0) \end{Bmatrix} \quad [3.2.11]$$

Once the initial values of λ_r and λ_θ are known, the primer vector can be computed at any time in the interval $[t_0, t_f]$ using equation (3.2.9). In obtaining the fuel optimal solution for a rendezvous between two orbits, the parameter optimization algorithm finds the optimum values for the initial and final coast angles. If the primer vector exceeds unity anywhere along a subarc, since the first two criteria due to Lion and Handelsmann are automatically satisfied, an additional impulse is considered.

If the number of impulses is greater than two and if the magnitude of the primer vector is less than unity along each subarc, the subarc is tested further for optimality at the intermediate impulse points. Over the trajectory, the Hamiltonian and the costate corresponding to the true anomaly λ_θ should be constant. Also the time derivative of the primer vector at the intermediate impulse point should be zero.

The procedure discussed thus far can be summarized as follows:

1. Check the magnitude of the primer vector on each subarc. If it is not less than unity, then the trajectory does not satisfy the necessary conditions for optimality.
2. If the magnitude of the primer vector is less than unity, and if the number of impulses is greater than two, the Hamiltonian, the costate λ_θ and the

time derivative of the primer vector are examined at the intermediate impulse point.

3.3 Examples

To verify the primer vector for the unconstrained problem, a coplanar rendezvous between two neighboring circular orbits was examined. This presents the most simple case of all rendezvous problems, and allows easy verification of known transfers.

An orbital rendezvous problem is characterized by many parameters. Even the most simple case of a circle-to-circle rendezvous problem involves at least four parameters. These are: outer to inner radius ratio, relative phase at the start of the maneuver, total time to rendezvous and the number of impulses permitted. For this study the variation with respect to the total-time-to-rendezvous only was examined for different number of impulses, while keeping the relative phase at the start of the maneuver constant and the radius ratio fixed.

A particular case of the above can be examined analytically. For unrestricted time Hohmann transfer is the optimal solution between two neighboring circular orbits, i.e. with outer to inner radius ratio less than or equal to 11.92. The transfer trajectory is an ellipse with its perigee radius equal to the inner orbit radius and the apogee radius equal to the outer orbit radius. The Hohmann

transfer time is the sum of the actual transfer time T_H and the phasing time T_ψ. These are given by:

$$T_H = \pi \sqrt{(\frac{a_T + a_{RV}}{2})^3} \qquad [3.3.1]$$

$$T_\psi = (\psi_i - \psi_H)\frac{T_s}{2\pi} \qquad [3.3.2]$$

where T_s is the synodic period given by

$$T_s = \frac{\pi T_{RV} T_T}{(T_T - T_{RV})} \qquad [3.3.3]$$

and ψ_H is the phase required for a Hohmann transfer given by :

$$\psi_H = \pi - \omega_T T_H \qquad [3.3.4]$$

where $T_T, \omega_T, T_{RV}, \psi_i$ are respectively the time period of the target, angular rate of the target, time period of the rendezvous vehicle RV and the phase difference of the target at the start of the maneuver.

Prussing [1969] has shown that using the linearized equations of motion, the primer vector has a unit magnitude on a Hohmann transfer between two neighboring orbits. However, using the nonlinear equations it is seen that primer vector has a magnitude close to unity. That this should be the case can be concluded by examining the primer vector component equations along the transfer subarc. A Hohmann transfer is characterized by two transverse impulses - one at perigee and the other at the apogee of the transfer ellipse. Consequently

$$\lambda_h(t_0) = -\frac{1}{r_p}$$
$$\lambda_h(t_f) = -\frac{1}{r_a} \qquad [3.3.5]$$

and

$$\lambda_v(t_0) = 0$$
$$\lambda_v(t_f) = 0 \qquad [3.3.6]$$

at the impulses. Therefore, from the expression for λ_v (A.11)

$$-\frac{\lambda_0 h}{e} + Cf(0) = 0$$
$$\frac{\lambda_0 h}{e} + Cf(\pi) = 0 \qquad [3.3.7]$$

and since $f(0) + f(\pi) \neq 0$, from (3.3.7) it follows that both λ_0 and C must be zero. Solving for D and B from the expression for λ_h given by (A.23), the costates λ_v and λ_h on the Hohmann transfer can be written as:

$$\lambda_v = -\frac{e}{2}\sin\theta$$
$$\lambda_h = \frac{e^2\sin^2\theta - 2(1 + e\cos\theta)}{2h^2} \qquad [3.3.8]$$

Therefore the primer vector magnitude on the Hohmann transfer can be written as

$$p = \sqrt{1 - \frac{e^2\sin^2\theta}{4(1 + e\cos\theta)^2}\{3 + 2e\cos\theta - e^2\}} \qquad [3.3.9]$$

Examining the above equation, it is seen that the second term is positive for all elliptic orbits. Consequently, the magnitude of the primer vector is less than unity over the entire transfer arc except at at the impulse points. Therefore, a Hohmann transfer between two circular orbits of arbitrary radius ratios, satisfies the first order necessary conditions for optimality.

For the case of restricted times, the parameter optimization algorithm was applied for various number of impulses and the results tested as described earlier.

3.4 Discussion

The two terminal orbits were taken to be in the same plane, with the non-maneuvering target in the outer orbit of radius r_a = 1.44 DU, and the rendezvous vehicle (RV) in the inner orbit of radius r_p = 1.2 DU. The objective was to verify and use the results of the Primer Vector Theory due to Lawden [1963] to indicate how many impulses are optimal for a particular space-flight maneuver.

To achieve and illustrate this, the total time of flight was varied from 22.31 TU to 5.43 TU, and the relative phase at the start of the maneuver was fixed at $\psi = \pi$ radians. The number of impulses was fixed *a priori* at 2, 3, ... and for a given initial guess the resulting solutions for a time limited rendezvous problem, (total time to rendezvous is less than or equal to a fixed time), was tested using the primer vector. The Hohmann transfer time to this problem

T_H = 19.912 TU. For a total time-to-rendezvous greater than this a Hohmann transfer was obtained, as might be expected since the problem considered is a time limited rendezvous as opposed to the time fixed rendevous.

For the fixed phase at the start of the maneuver, the variation of the cost function with respect to the total time-to-rendezvous is examined for a different number of impulses. It can be observed that for a fixed number of impulses, the cost function increases monotonically as shown in figure 2 as the time to rendezvous decreases. For very large total time-to-rendezvous, when the time limited problem behaves as a free time problem, a Hohmann transfer is obtained with a total time-to-rendezvous = 19.912 TU. For all total time-to-rendezvous greater than that required for a Hohmann transfer, all multiple impulse trajectories collapse (i.e. some of the impulses become near zero) to the Hohmann transfer.

While examining the fuel-optimal orbital rendezvous trajectories, it is seen that the solutions obtained from the parametric optimization method yield only locally optimal solutions as these are dependent on the initial guess values of the parameters. For instance, whereas for a time free problem a Hohmann transfer is obtained, with a different initial guess the algorithm converged to a different solution which, however, did not satisfy the necessary conditions in terms of the primer vector conditions. Often in obtaining the candidate trajectories by varying total time-to-rendezvous, two solutions with entirely different characteristics may be obtained for a small change in time. For example, in the circle-to-circle rendezvous problem considered at time t = 14.87 TU trajectories belonging to

entirely different family of curves, with a large difference in the cost function were found, as shown in figure 2. Interestingly enough, the trajectory yielding the higher cost function satisfies all the primer vector necessary conditions for an optimum, thus indicating that this trajectory might indeed be a local minimum.

On the trajectory which yielded the lower cost function, the magnitude of the primer vector exceeded unity. According to the criterion due to Lion and Handelsmann for non-optimal trajectories, a decrease in the cost function could be effected by considering an additional impulse. This impulse should be applied at a point where the primer vector attains its maximum magnitude and in a direction opposite to the primer vector direction at that point. However, with the introduction of an additional impulse, the problem itself is changed and hence such a strategy can be used only as a good starting guess.

To obtain the solution using parameter optimization technique, it is advisable to supply as an initial guess a set of parameters which satisfies the rendezvous constraint. However, by using the criteria due to Lion and Handelsmann which determines the direction of the impulse, a rendezvous can be achieved only by varying the time of flight on the two subarcs. This may not always be possible and the computational procedure required to determine the magnitude of the change in velocity needed and the time of flight on each of the subarcs is very complicated and not justified for generating only an initial guess for the parameter optimization method. Hence, in this study, at the location where the primer vector attains its maximum, a small (arbitrary) impulse is added to

generate the next initial candidate trajectory which satisfies all rendezvous constraints. The resulting solution satisfied the necessary optimality conditions.

The three impulse trajectories yield a lower value for the cost function in comparison to the two impulse trajectories as shown in figure 2. As the total time-to-rendezvous is reduced, a four impulse trajectory with a lower cost function evolved. With further reduction in the total time-to-rendezvous, the angle of coast on one of the subarcs in the four impulse trajectory collapses to the prescribed minimum, thus yielding a three impulse trajectory. This new three impulse trajectory obtained belongs to a different family of three impulse trajectories from that obtained earlier. Sample trajectories belonging to both families are shown in figures 3 and 4.

To further illustrate the primer vector theory, a limited time rendezvous problem between two coplanar non-coaxial ellipses is considered. The outer orbit was characterized by the following orbital elements : semi-major axis $a_t = 2.0$, eccentricity $e_t = 0.1$, inclination $i_t = \frac{\pi}{4}$, node $\Omega_t = 0$, argument of the perigee $\omega_t = \frac{\pi}{4}$, and the inner orbit was characterized by the following orbital elements : semi-major axis $a_i = 1.4$, eccentricity $e_i = 0.2$, inclination $i_i = \frac{\pi}{4}$, node $\Omega_i = 0$, argument of the perigee $\omega_i = 0$. Since Hohmann type transfers are impossible for this problem, it is not known beforehand whether two impulses are sufficient for the time free problem. As before, two impulse trajectories were examined and the variation of the cost function with respect to total time-to-rendezvous was examined. For the time free problem, two different two impulse trajectories were found with different

transfer times and with a large difference in the cost function. One trajectory obtained entails coasting on the initial orbit, an impulse leading to an intercept course with the target and a final impulse providing the velocity match (figure 5). The other trajectory obtained involves an outward impulse without an initial coast, yielding a near rectilinear orbit (figure 6). The primer vector histories (figure 7 and 8) were examined for both these trajectories to check for optimality. As is evident from the figure, though the rectilinear trajectory yields a higher cost function value, it satisfies the first order necessary conditions due to Primer Vector Theory. However, for the other trajectory, the primer vector history fails to satisfy the first order necessary conditions for optimality. Therefore, by applying the criterion due to Lion and Handelsmann, a three-impulse trajectory (figure 9) yielding a lower cost function value was found, with a primer vector magnitude history satisfying the first order necessary conditions for optimality. As can be seen, the peak of the primer vector history for the non-optimal two-impulse trajectory occurs close to the point of application of the second impulse in figure 10.

The variation of the cost function with respect to the total time-to-rendezvous is shown in figure 11. A four impulse trajectory was not found computationally. However, this does not exclude their existence.

4.0 Constrained Problem

4.1 Introduction

Orbital transfers always occur in the presence of an attracting body with a finite radius; consequently any physically possible trajectory should not pass through the body. The analysis carried out so far does not incorporate this constraint. Absence of the radial constraint in the set of assumptions is justified for those trajectories where the minimum-radius constraint is not encountered. Often, it is observed that when orbital transfers close to the attracting body are considered, the unconstrained solution results in a trajectory which passes through the body. To avoid such trajectories, it is necessary to include the radial constraint in the analysis. However, the trajectory obtained in this case may contain subarcs which either touch or coincide with the constraint arc. Over these subarcs, the analysis carried out in the previous chapters is not applicable.

In this chapter, the problem is reformulated with the radial constraint in the form of a state-inequality constraint and conclusions are drawn from the Minimum Principle.

4.2 *Necessary Conditions*

The radial constraint can be written in the form of a state-inequality as:

$$S = R_0 - r \leq 0 \qquad [4.2.1]$$

where R_0 is the specified minimum radius that should not be violated by the optimal trajectory. To formulate the problem for a minimum fuel rendezvous between two orbits, the procedure described by Bryson and Ho [1975] is used. Successive total time derivatives of (4.2.1) are found until the control variable appears explicitly. If q total time derivatives are required then it is called the q^{th} order state variable inequality constraint. For this problem the control variable appears explicitly in the second time derivative.

$$\dot{S} = - v \qquad [4.2.2]$$

$$\ddot{S} = - \left(\frac{h^2}{r^3} - \frac{1}{r^2} + \frac{c \beta l_r}{m} \right) \qquad [4.2.3]$$

The second total time derivative of the radial constraint given by (4.2.3), is added on with an appropriate multiplier $\gamma(t)$ to the Hamiltonian given by equation (2.3.2) yielding:

$$H = \lambda_r v + \lambda_\theta \frac{h}{r^2} + \lambda_v \left(\frac{h^2}{r^3} - \frac{1}{r^2} + c\beta\frac{l_r}{m}\right) + \lambda_h r c \beta \frac{l_\theta}{m} - \lambda_m \beta + \mu(l_r^2 + l_\theta^2 - 1) - \gamma\left(\frac{h^2}{r^3} - \frac{1}{r^2} + \frac{c\beta l_r}{m}\right) \qquad [4.2.4]$$

where $\lambda_r, \lambda_\theta, \lambda_v, \lambda_h$ and λ_m are given by the following costate equations :

$$\dot{\lambda}_r = 2\lambda_\theta \frac{h}{r^3} + (\lambda_v - \gamma)\left(\frac{3h^2}{r^4} - \frac{2}{r^3}\right) - \lambda_h c \beta \frac{l_\theta}{m} \qquad [4.2.5]$$

$$\dot{\lambda}_\theta = 0 \qquad [4.2.6]$$

$$\dot{\lambda}_v = -\lambda_r \qquad [4.2.7]$$

$$\dot{\lambda}_h = \frac{-\lambda_\theta}{r^2} - \frac{2(\lambda_v - \gamma)h}{r^3} \qquad [4.2.8]$$

$$\dot{\lambda}_m = [(\lambda_v - \gamma) l_r + \lambda_h r l_\theta] \frac{c\beta}{m^2} \qquad [4.2.9]$$

From the Minimum Principle, the control variables l_r , l_θ and β are chosen so as to satisfy :

$$(\lambda_v - \gamma)\frac{c\beta}{m} + 2\mu l_r = 0 \qquad [4.2.10]$$

$$r\lambda_h \frac{c\beta}{m} + 2\mu l_\theta = 0 \qquad [4.2.11]$$

and the thrust magnitude β is such that it minimizes the Hamitonian H.

$$M(\underline{\lambda}, \underline{x}) = \min_{\beta} \{ [((\lambda_v - \gamma) l_r + r \lambda_h l_\theta) \frac{c}{m} - \lambda_m] \beta \} + \lambda_r v + \lambda_\theta \frac{h}{r^2} + (\lambda_v - \gamma) (\frac{h^2}{r^3} - \frac{1}{r^2}) \quad [4.2.12]$$

Define two vectors

$$\bar{p} \equiv \{\lambda_v - \gamma, r \lambda_h\} \quad [4.2.13]$$

$$\hat{e} \equiv \{l_r, l_\theta\} \quad [4.2.14]$$

where $\bar{p}$ is referred to as the **primer vector.** The equation [4.2.12] can be rewritten as

$$M(\underline{\lambda}, \underline{x}) = \min_{\beta} \{ [(\bar{p} \cdot \hat{e}) \frac{c}{m} - \lambda_m] \beta \} + \lambda_r v + \lambda_\theta \frac{h}{r^2} + (\lambda_v - \gamma) (\frac{h^2}{r^3} - \frac{1}{r^2}) \quad [4.2.15]$$

Therefore for a non-zero thrust magnitude the minimum value is obtained when $\bar{p} \cdot \hat{e} = -p$, where p is the norm of $\bar{p}$. Using this in equations (4.2.10) and (4.2.11) the components of the primer vector are obtained as:

$$\lambda_v - \gamma = - l_r p \quad [4.2.16]$$

$$r \lambda_h = - l_\theta p \quad [4.2.17]$$

As defined before for an unconstrained problem, a switching function can be defined as

$$\sigma = -\frac{c\,p}{m} - \lambda_m \qquad [4.2.18]$$

with similar properties.

In a typical problem with the radial constraint introduced as described above, three possibilities exist :

1. The radial constraint is not active, i.e. the trajectory does not encounter the constraint.
2. Some of the subarcs touch the radial constraint.
3. Some of the subarcs follow the contraint arc. This is possible since the constraint arc is a valid solution to equations of motion.

In the event none of the subarcs either touch or ride the constraint arc, the entire analysis can be carried out as for an unconstrained problem. But if either of the other possibilities arises, the analysis needs to be carried out in a different manner.

For problems with state variable inequality constraints, costate variables can not be determined uniquely on the constraint arc. Assuming the tangency condition

$$\begin{aligned} S &= 0 \\ \dot{S} &= 0 \end{aligned} \qquad [4.2.19]$$

to hold at the entry point to the constraint arc, a jump condition should be satisfied by the costates:

$$\lambda(t_{en}^{+}) = \lambda(t_{en}^{-}) - \mu_0 S_x(x(t_{en}^{-})) - \mu_1 \dot{S}_x(x(t_{en}^{-})) \qquad [4.2.20]$$

The constant μ_0 is unique, but an arbitrary constant could possibly be added to μ_1. This, however, causes a discontinuity in the costates at the exit point. Therefore, by requiring the continuity of the costates at the exit point to the constraint arc, the uniqueness in the jumps in the costates can be ensured. Therefore by applying equation (4.2.20) to each of the costate variables the following jump conditions can be determined:

$$\lambda_r(t_{en}^{+}) = \lambda_r(t_{en}^{-}) + \mu_0 \qquad [4.2.21]$$

$$\lambda_v(t_{en}^{+}) = \lambda_v(t_{en}^{-}) + \mu_1 \qquad [4.2.22]$$

The remaining costates do not experience a discontinuity at the entry and the exit points. On an optimal trajectory the constant multipliers μ_0 and μ_1 must satisfy the following necessary conditions, as given by Kreindler [1982]:

$$\begin{aligned} \mu_0 + \dot{\gamma}(t_{en}) &\geq 0 \\ \mu_1 - \gamma(t_{en}) &= 0 \end{aligned} \qquad [4.2.23]$$

$$\begin{aligned} \mu_0 &\geq 0 \\ \mu_1 &\geq 0 \end{aligned} \qquad [4.2.24]$$

From the geometry of the trajectories, it can be seen that a touch point can occur only at the perigee of the orbit. Therefore from the requirement of continuity of the Hamiltonian across the the touch point, it can be seen that across a touch

point the costate corresponding to the radial velocity λ_v is continuous. Hence, on a touch point arc μ_1 is zero.

Since the switching function is negative on the coasting arc, the primer vector must have a magnitude less than unity over a coasting arc.

4.3 Computational Procedure

Parameter optimization scheme used before can be used to obtain rendezvous trajectories for the radial constraint problem for a given number of impulses. This is done by including the minimum radius constraint as an additional inequality constraint. As before, in obtaining a candidate fuel-optimal trajectory, it is not known *a priori* how many impulses are needed and whether or not the chosen number of impulses truly provide an optimum. In response to these questions, the primer vector theory developed in the preceding chapters and sections can provide some answers. It can show whether or not the trajectories obtained are at least locally optimal.

To verify the candidate trajectories obtained from parameter optimization, the costate variables and the primer vector have to be computed. Costates on an unconstrained subarc can be evaluated using methods described in the previous chapters. For constrained problem, a procedure is required to provide the costates at any time t along the touch point arc and the constraint arc. In computing the costates along either touch point arcs or constraint arcs, jumps in

the costates λ_r and λ_v at the entry point to a constraint arc and the jump in λ_r across the touch point on a touch point subarc should also be evaluated. Therefore, the number of unknown quantities on each of these types of arcs are different. Consequently, a different procedure must be used to compute the costates and the jumps on each type of arc.

4.3.1 Constraint Arc

Consider a trajectory which includes a constraint arc of finite length (figure 12). The trajectory comprises of a sequence of conic section coasting arcs with impulses in between them. From the geometry of the arcs, it is obvious that a transfer between two points not equidistant from the focal point is not possible with a circular arc. Therefore, for a transfer from one orbit to an intermediate circular constraint arc and after traversing for a finite non-zero time duration on the constraint arc onto the final orbit requires at least two unconstrained non-circular conic section arcs. Considering the junction between any two arcs as a point of application of an impulse, it is observed that a minimum of four impulses are required. Hence, a typical transfer trajectory consists of: an impulse to get onto an "unconstrained" arc leading to the constraint arc, an impulse to get onto the constraint arc, coast on the constraint arc for a finite time duration, an exit impulse to get on to another unconstrained arc, a coast along the "unconstrained" sub arc on an intercept course and the final impulse providing the rendezvous.

Geometrically, the end point of the subarc leading to the constraint arc and likewise the starting point of the subarc leading from the constraint arc lies on the constraint surface, at which location an impulse is applied. Therefore, one is more inclined to think of this arc as a special kind of touch point arc. However, in the analysis, if this point is excluded from the subarc, the subarc can be viewed as an unconstrained arc. Therefore, the costates can be computed using the procedure described in the previous chapter.

Consider the constraint-arc-segment of the trajectory. Let $[t_{en}, t_{ex}]$ define the traversing interval on the constraint arc. Across an impulse, the costate corresponding to the true anomaly λ_θ does not vary. It also does not experience a jump at the entry point to the constraint arc, as can be inferred from equation (4.2.20). Thus, from either of the non-constraint arcs, λ_θ is known. Since the primer vector has a unit magnitude at an impulse, at $t = t_{en}$, $r\lambda_h$ has a value equal to the negative of the transverse direction cosine of the thrust vector, as given by (4.2.17). Assuming tangency conditions at the exit point of the constraint arc, i.e. at $t = t_{ex}$ the costates λ_v and λ_h can be determined from (4.2.16) and (4.2.17). Since the constraint arc is also a coasting arc, from the solution of the costate equations, the Transition matrix can be evaluated at $t = t_{ex}$, and partitioned to yield the expressions for λ_v and λ_h as:

$$\begin{Bmatrix} \lambda_v(t_{ex}) \\ \lambda_h(t_{ex}) \end{Bmatrix} = \begin{bmatrix} \varphi_{3\,1}(t_f) & \varphi_{3\,2}(t_f) & | & \varphi_{3\,3}(t_f) & \varphi_{3\,4}(t_f) \\ \varphi_{4\,1}(t_f) & \varphi_{4\,2}(t_f) & | & \varphi_{4\,3}(t_f) & \varphi_{4\,4}(t_f) \end{bmatrix} \begin{Bmatrix} \lambda_r(t_{en}) \\ \lambda_\theta(t_{en}) \\ \lambda_v(t_{en}) \\ \lambda_h(t_{en}) \end{Bmatrix} \qquad [4.3.1]$$

$\lambda_r(t_{en})$ and $\lambda_v(t_{en})$ can be computed as :

$$\begin{Bmatrix} \lambda_r(t_{en}) \\ \lambda_v(t_{en}) \end{Bmatrix} = \begin{bmatrix} \varphi_{3\,1}(t_f) & \varphi_{3\,3}(t_f) \\ \varphi_{4\,1}(t_f) & \varphi_{4\,3}(t_f) \end{bmatrix}^{-1} \begin{Bmatrix} \lambda_v(t_{ex}) - \varphi_{3\,2}(t_f)\,\lambda_\theta(t_{en}) - \varphi_{3\,4}(t_f)\,\lambda_h(t_{en}) \\ \lambda_h(t_{ex}) - \varphi_{4\,2}(t_f)\,\lambda_\theta(t_{en}) - \varphi_{4\,4}(t_f)\,\lambda_h(t_{en}) \end{Bmatrix} \quad [4.3.2]$$

Since the magnitude of the primer vector is unity at an impulse, the multiplier $\gamma(t_{en})$ can be computed from equation (4.2.16) as:

$$\gamma\,(t_{en}) \;=\; \lambda_v + l_r \qquad [4.3.3]$$

For a candidate trajectory with constraint arc, γ should be positive along the constraint arc, as given by (4.2.23). Also on such an arc the Hamiltonian H and the costate λ_θ should be constant. However, there are not enough conditions known yet to determine the variation of the multiplier $\gamma(t)$ along the constraint arc. Therefore, a procedure to compute the primer vector on a constraint arc is not provided.

4.3.2 Touch Point Arcs

Now consider a trajectory which includes a touch point subarc (figure 13). A touch point subarc can be described as a coasting arc such that its perigee radius equals the minimum radius. In this case the entire trajectory can be composed of a sequence of touch point subarcs, or sequence of touch point and unconstrained subarcs or a combination thereof. Unlike the unconstrained

problem where the entire trajectory was viewed as a sequence of two impulse trajectories and the costates and Hamiltonian computed on each segment separately, the touch point problem must be considered in its entirety.

At a touch point, the costate λ_r experiences a jump as shown by equation (4.2.21). On such an arc, there is one more unknown than the corresponding unconstrained two impulse trajectory and the number of boundary conditions available appear to be the same. Therefore, an attempt is made to choose a set of costates and the jump in λ_r at the touch point which satisfies all necessary conditions on a two impulse touch point trajectory. The procedure adopted here is to use a one-dimensional search method [ref. Johnson and Kamm, 1973] to find a jump in λ_r which would make the magnitude of the primer vector less than unity over the entire arc except at the impulse points where it is forced to be unity. If the jump obtained is positive, the trajectory is " considered to satisfy " the necessary conditions.

For multiple-impulse touch point trajectories, if at least one of its subarcs is unconstrained, then the costates and the jump in λ_r at the touch point can be computed " uniquely " within a scalar constant multiplier. If a touch point arc starting at $t = t_0$ and ending at $t = t_f$, with the touch point at $t = \hat{t}$ is considered, the touch point subarc can be viewed as two separate subarcs - one leading to and the other leading from the touch point. The costates can be expressed in terms of transition matrices Φ_I and Φ_{II} computed over each of the part of the subarc, i.e.

$$\underset{\sim}{\lambda}_I = \Phi_I\ (t_0, t)\ \lambda_0 \qquad \textit{for}\ t_0 \le t \le \hat{t}$$

and

$$\underset{\sim}{\lambda}_{II} = \Phi_{II}\ (\hat{t}, t)\ \hat{\underset{\sim}{\lambda}} \qquad \textit{for}\ \hat{t} \le t \le t_f$$

Also at $t = \hat{t}$

$$\hat{\lambda} = \underset{\sim}{\lambda}_I(\hat{t}) + \underset{\sim}{\mu}$$

where $\underset{\sim}{\mu} = \{\mu_0\ 0\ 0\ 0\}$. Therefore

$$\underset{\sim}{\lambda}(t_f) = \Phi_{II}(\hat{t}, t_f)\ \Phi_I(t_0, \hat{t})\ \lambda_0 + \Phi_{II}(\hat{t}, t_f)\ \underset{\sim}{\mu}$$

This can be written in the matrix notation by rearranging the equations for $\lambda_v(t_f)$ and $\lambda_h(t_f)$ to yield two linear equations in terms of $\lambda_r(t_0)$, $\lambda_\theta(t_0)$ and the jump μ_0 and defining $\Psi = \Phi_{II}(\hat{t}, t_f)\ \Phi_I(t_0, \hat{t})$

$$\begin{bmatrix} \Psi_{3,1} & \Psi_{3,2} & \Phi_{II_{3,1}} \\ \Psi_{4,1} & \Psi_{4,2} & \Phi_{II_{4,1}} \end{bmatrix} \begin{Bmatrix} \lambda_r(t_0) \\ \lambda_0(t_0) \\ \mu_0 \end{Bmatrix} = \begin{bmatrix} \lambda_v(t_f) - \Psi_{3,3}\lambda_v(t_0) - \Psi_{3,4}\lambda_h(t_0) \\ \lambda_h(t_f) - \Psi_{4,3}\lambda_v(t_0) - \Psi_{4,4}\lambda_h(t_0) \end{bmatrix}$$

In order to evaluate the unknowns, a third equation is required. Now, the value of the Hamiltonian is known from the unconstrained subarcs. This can be used to yield the required third equation as:

$$\begin{bmatrix} v & \frac{h}{r^2} & 0 \end{bmatrix} \begin{Bmatrix} \lambda_r(t_0) \\ \lambda_\theta(t_0) \\ \mu_0 \end{Bmatrix} = H$$

This set of linear equations can be solved simultaneously to yield the initial values of λ_r and λ_θ and the jump in λ_r at the touch point. The candidate trajectory satisfies the necessary conditions only if the magnitude of the primer vector is less than unity over each of the transfer subarcs and the jump μ_0 is positive. The costate λ_θ and the Hamiltonian should be constant over the entire trajectory.

In the event all coasting subarcs are touch point arcs, the number of variables seem to exceed the number of equations to determine them. On trajectories which include at least one unconstrained arc, the Hamiltonian and the costate λ_θ are known. However, neither of these are known on the trajectories comprising of only touch point subarcs, and so some other means must be used to determine the costates and the jumps in λ_r at the touch point. To this intent, two procedures are proposed.

A one-dimensional procedure is used to determine a positive jump in λ_r on any one subarc which would yield a primer vector time history less than unity on the subarc except at the impulse points. Hence, the Hamiltonian is known from this and thereon the procedure described for trajectories involving touch point arcs and unconstrained arcs can be used to determine the costates and the jumps in λ_r on the remaining subarcs. If these jumps are also positive and if the

costate λ_θ is a constant over the entire trajectory, then the given trajectory satisfies the necessary optimality conditions.

Another method would be to use parameter optimization to determine the jumps in λ_r at the touch points. The procedure is to set up a parameter optimization problem which minimizes the sum of the squares of the difference in the Hamiltonian at the point of application of an impulse with respect to the jumps in the costate λ_r . A constraint is included in the procedure which would ensure that the jumps are positive. On computation of the jumps, the costates on each subarc are computed. If the Hamiltonian and the costate λ_θ are constant over the entire trajectory, and if the magnitude of the primer vector is less than unity over the entire subarc except at an impulse, then the given trajectory satisfies the necessary optimality conditions.

4.4 Examples and Discussions

To verify and illustrate the primer vector theory incorporating the radial constraints the circle-to-circle rendezvous problem is considered. The radial constraint was included as an inequality constraint in the parametric optimization code. Solution obtained is then tested against the necessary conditions for optimality. The nature of the transfer is examined for various total time-to-rendezvous.

Consider a two impulse trajectory. In the absence of any total time-to-rendezvous restrictions, a Hohmann transfer is obtained. This is so since these transfers are optimal for transfers between neighboring orbits and also do not violate the radial constraint [ref. Marec,1979]. To illustrate the primer vector theory numerically, a radial constraint $R_0 = 1$ DU was chosen and the time for transfer systematically reduced. It was found that the pattern of optimal trajectories obtained is similar to that obtained for the unconstrained problem until the short time-to-rendezvous causes the constraint to become active. For the example chosen, the three impulse transfer is optimal until one of its subarcs becomes a touch point arc. As the total time-to-rendezvous is reduced further, the four impulse transfer becomes optimal in the primer vector sense. Here the transition from an unconstrained problem to the constrained problem occurred with its second subarc becoming a constraint arc. This change from a unconstrained problem to one with a constraint arc is not generally true. For instance, if the minimum radius is increased then for a certain time-to-rendezvous one of the subarcs contains a touch point, and this may gradually become a constraint arc as the total time is reduced further. In some cases an additional impulse might become necessary. Because of computational difficulties, trajectories with the number of impulses greater than four were not found.

The effect of the minimum radius on the cost function for a fixed total time-to-rendezvous and relative phase at the beginning of the maneuver was examined, refer figures 14, 15 and 16. A known optimal three impulse solution for the unconstrained problem was chosen and the minimum radius was fixed at

a value equal to the minimum radius encountered in the trajectory. This is the optimal trajectory for the problem, which now also includes a touch point in one of its subarcs. By letting the minimum radius encountered in the trajectory to be equal to R_0 the trajectory becomes the transition solution between an unconstrained and a constrained problem. Therefore, on such an arc, since it was tailored to be so, the jump in the costate λ_r at the touch point is zero. As seen from figures 15 and 16, when the value of the minimum radius constraint is increased, the payoff increases monotonically. On these three impulse trajectories, though the jump in the costate λ_r was found to be positive, the magnitude of the primer vector exceeded unity indicating that it is non-optimal. For each of these minimum radius constraint values a four impulse trajectory was found with better payoff and which satisfied the necessary conditions for optimality. As the minimum radius was increased further, the magnitude of the primer vector on one of the subarcs of a four impulse trajectory exceeded unity. This indicates that an additional impulse may be required. For a different total time-to-rendezvous, touch point subarc in the four impulse trajectory gradually evolved into a constraint arc before becoming non-optimal for a further increase in the minimum radius constraint.

Since the number of parameters which characterize the orbital rendezvous problem in the presence of a radial constraints is fairly high, it is difficult to draw any general conclusions. However, for the present example, some interesting observations can be made. The two impulse trajectories were found in general to be non-optimal. However, certain two impulse trajectories satisfying the

necessary conditions for optimality were found. As the total time-to-rendezvous was decreased, these converged to a degenerate conic. If the total time-to-rendezvous is reduced further, no solutions belonging to this family of trajectories could be found.

Three impulse trajectories were found to be optimal only as long as the radial constraint was not active. A four impulse trajectory which satisfied all necessary conditions for an optimum, could always be found when the constraint was active. If the total time-to-rendezvous is reduced further, five or more impulses may be required, however such trajectories could not be computed due to numerical difficulties.

By examining the trajectories, it was found that trajectories with two consecutive touch points were in general non-optimal as a trajectory with one or more additional impulses could be found computationally yielding a lower cost function. Also, the new candidate trajectory was found to satisfy the necessary conditions for optimality.

5.0 Summary

In this study, Lawden's Problem is reformulated using polar coordinates to describe the equations of motion and the necessary conditions for optimality are rederived from the Minimum Principle. Trajectories obtained using the parameter optimization are then tested for optimality against these necessary conditions. If a trajectory fails to satisfy the necessary conditions, then the criterion due to Lion and Handelsmann is used to generate the optimal trajectory.

Numerical solutions show that with decrease in total time-to-rendezvous the cost function increases monotonically. It is observed that in general three or more impulse trajectories yield a lower cost function. A large number of locally optimal solutions belonging to different family of curves were also found.

Lawden's Problem is then reformulated incorporating the radial constraint. Necessary conditions for optimality are then obtained from the Minimum Principle. Numerical procedures are provided to compute the costates and the Hamiltonian along the touch point arc and the constraint arc. The patterm of

transfer trajectories obtained is similar to that obtained for the unconstrained problem, until the constraint becomes active.

For a certain total time-to-rendezvous, trajectories comprising of only touch-point arcs are found. For this total time, a trajectory with an additional impulse, including an unconstrained subarc could be found with a lower cost function. This was found to satisfy the necessary conditions also. More than four impulses are found to be need trajectoriee cases. However, these were not found computationally because c, until the al problems. For non-optimal trajectories, the criterion due to Lion and Handelsmann was used successfully to generate optimal trajectories for the fuel-optimal rendezvous problems.

Several extensions to this are apparent, most obvious being to consider three dimensiona maneuvers. Another possible extension is to examine fuel optimal maneuvers in the presence of an oblate attracting body.

References

1. Bate, R.R., Mueller, D.D. and White, J.E., *Fundamentals of Astrodynamics.*,Dover Publications, Inc.,New York, 1971.

2. Bryson, A.E. and Ho, Y.C. *Applied Optimal Control*, Revised Printing, New York, New York, 1975.

3. Chiu, J.-H., *Optimal Multiple-Impulse Nonlinear Orbital Rendezvous*, Ph.D. Thesis, University of Illinois at Urbana-Champaign, 1984.

4. Chiu, J.-H. and Prussing, J.E., " Optimal Multiple-Impulse Time-Fixed Rendezvous Between Circular Orbits," *Journal of Guidance, Control and Dynamics*, pp.17-22, Jan-Feb 1986.

5. Das, A., Cliff, E.M. and Kelley, H.J., "An Active-Constraint Logic for Non-Linear Programming," *Optimal Control Applications & Methods*, pp.221-234, 1984.

6. Edelbaum, T.N.,"How many Impulses ?," *Astronautics and Aeronautics*, pp.64-69, Nov 1967.

7. Glandorf, D.R., *Optimal Fixed-Time Orbital Transfer with a Radial Constraint*, Ph.D. Thesis, Iowa State University, 1967.

8. Gobetz, F.W. and Doll, J.R.,"A Survey of Impulsive Trajectories," *AIAA Journal*, pp.801-834, 1969.

9. Hoelker, R.F. and Silber, R., "The bi-elliptical transfer between coplanar circular orbits," *Advances in Ballistic Missiles and Space Technology*, Vol. 3, Pergamon, Oxford, pp.164, 1961.

10. Johnson, I.L., Kamm, J.L., "Accelerating One-Dimensional Searches," *AIAA Journal*, pp.757-759, May 1973.

11. Kelley, H.J., Lefton, L. and Johnson, I.L., " Curvilinear Projection Developments," *Journal of Guidance and Control*, Vol.1, pp.80-82, Jan-Feb 1978.

12. Kreindler, E.,"Additional Necessary Conditions for Optimal Control with State Variable Inequality Constraints, " *JOTA*, pp. 241-250, Oct 1982.

13. Kwakernaak, H. and Sivan, R., *Linear Optimal Control Systems*, Wiley-Interscience, New York, 1972.

14. Lawden, D.F., "Interplanetary Rocket Trajectories.," *Advances in Space Sciences*, Chap. 1, Academic Press, New York, 1959.

15. Lawden, D.F., "Optimal Intermediate Thrust Arcs in a Gravitational Field.," *Astronautica Acta*, pp.106-123, 1962.

16. Lawden, D.F. *Optimal Trajectories for Space Navigation*, Butterworths, London, 1963.

17. Lefton, L. and Kelley, H.J., *Variable-Metric Projection Optimization Program Notes*, Report No. 77-12, Contract NAS 1-14891, July 1978.

18. Lion, P.M. and Handelsmann, M., "Primer Vector on a Fixed-Time Impulsive Trajectories," *AIAA Journal*, pp.127-132, Jan 1968.

19. Lutze, F.H., Cliff, E.M. and Kelley, H.J., *Optimal Rendezvous with Cooperative Vehicles II*, VPI&SU Report, July 1985.

20. Marec, J.P., *Trajectoires Spatiales Optimales*, Cours de l'ENSAE, Toulouse, 1973.

21. Marec, J.P., *Optimal Space Trajectories*, Elsevier, New York, New York, 1979.

22. Neustadt, L.W., "Optimization, A Moment Problem and Nonlinear Programming," *SIAM Journal on Control*, pp.33-53, 1964.

23. Neustadt, L.W., "A General Theory of Minimum-Fuel Space Trajectories," *SIAM Journal on Control*, pp.317-356, 1966.

24. Potter, J.E. and Stern, R.E., "Optimization of Midcourse Velocity Corrections," *Proceedings IFAC Symposium on Automatic Control in the*

Peaceful Uses of Space, Stavanger, Norway, Plenum Press, N.Y., pp.70-84, June 1965.

25. Prussing, J.E., "Optimal Four Impulse Fixed-Time Rendezvous in the Vicinity of a Circular Orbit," *AIAA Journal*, pp.928-935, May 1969.

26. Prussing, J.E., "Optimal Two and Three Impulse Fixed-Time Rendezvous in the Vicinity of a Circular Orbit," *AIAA Journal*, pp.1221-1228, July 1970.

27. Robbins, H.M., "Optimality of Intermediate-Thrust Arcs of Rocket Trajectories," *AIAA Journal*, pp.1094-1098, June 1965.

28. Robbins, H.M., "An Analytical Study of the Impulsive Approximation," *AIAA Journal*, pp.1417-1423, Aug 1966.

Figures

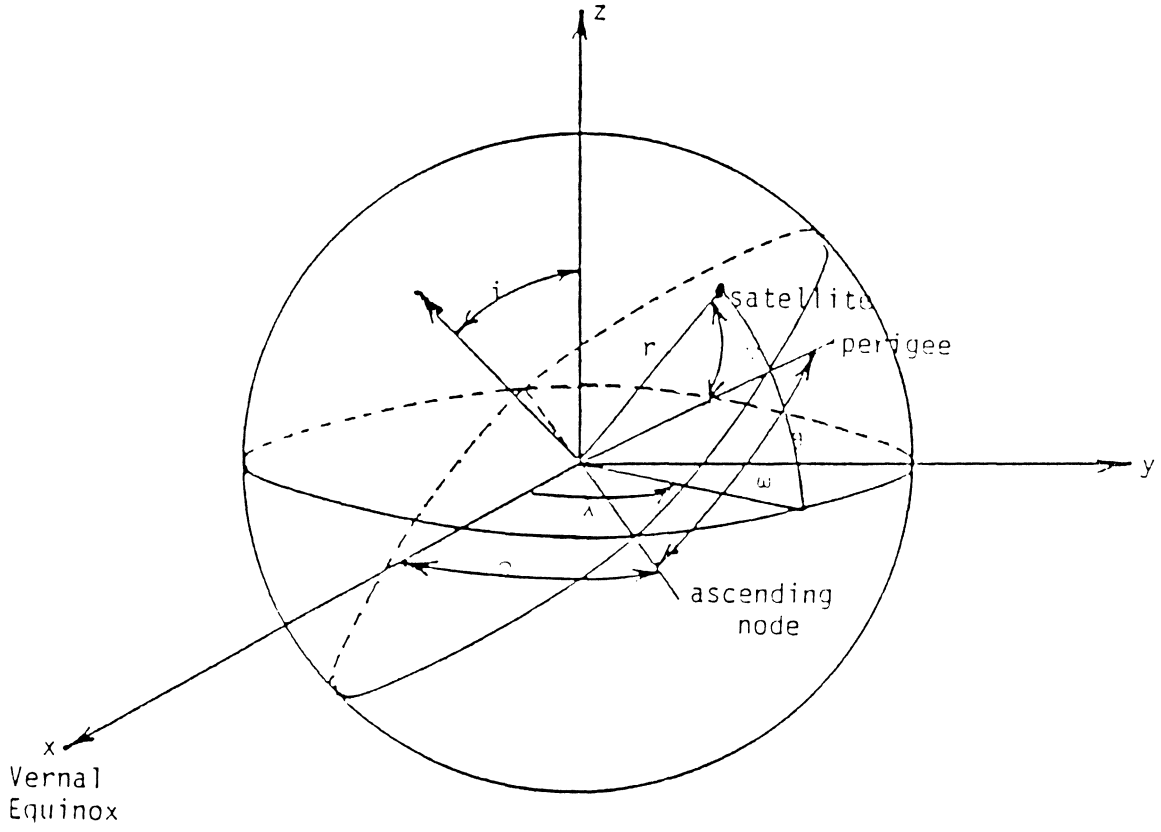

Figure 1. Geometry of Orbit.

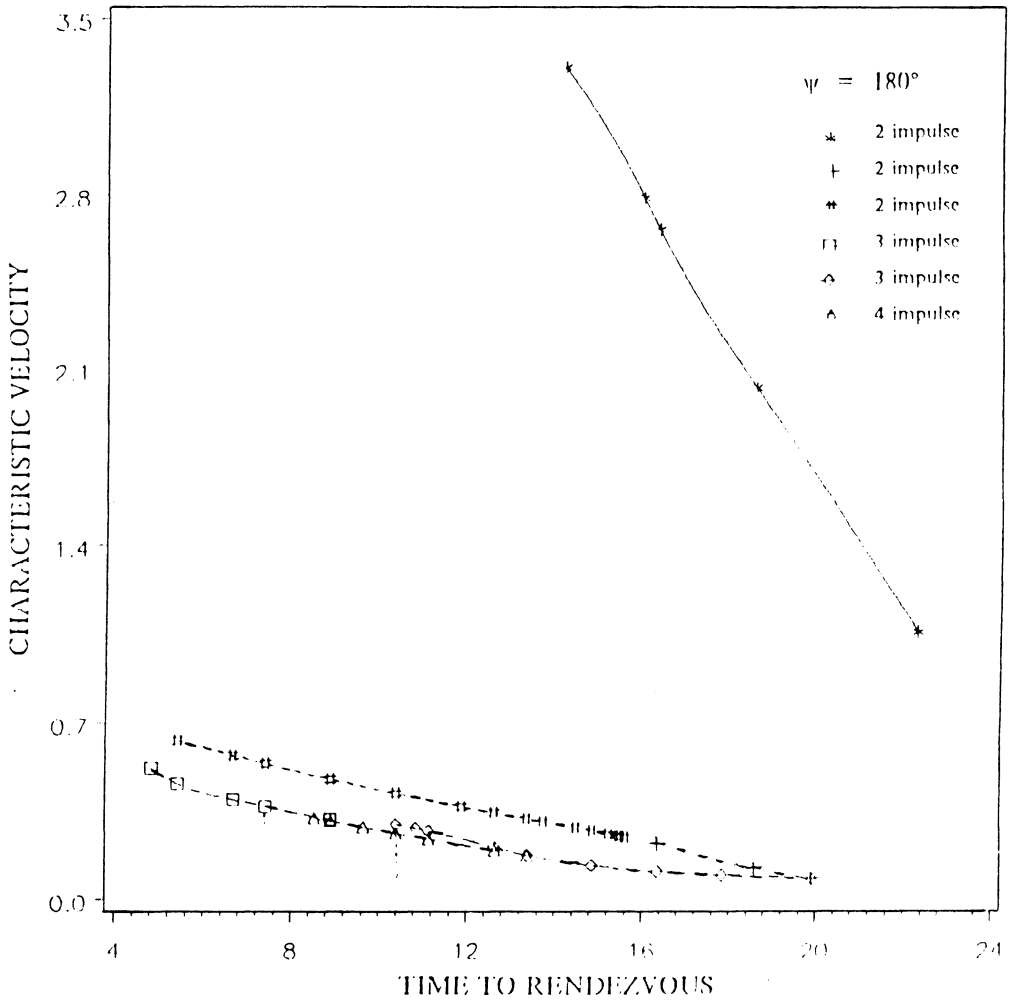

Figure 2. Variation of the Characteristic Velocity with total time for Unconstrained Circle-to-Circle Rendezvous Problem.

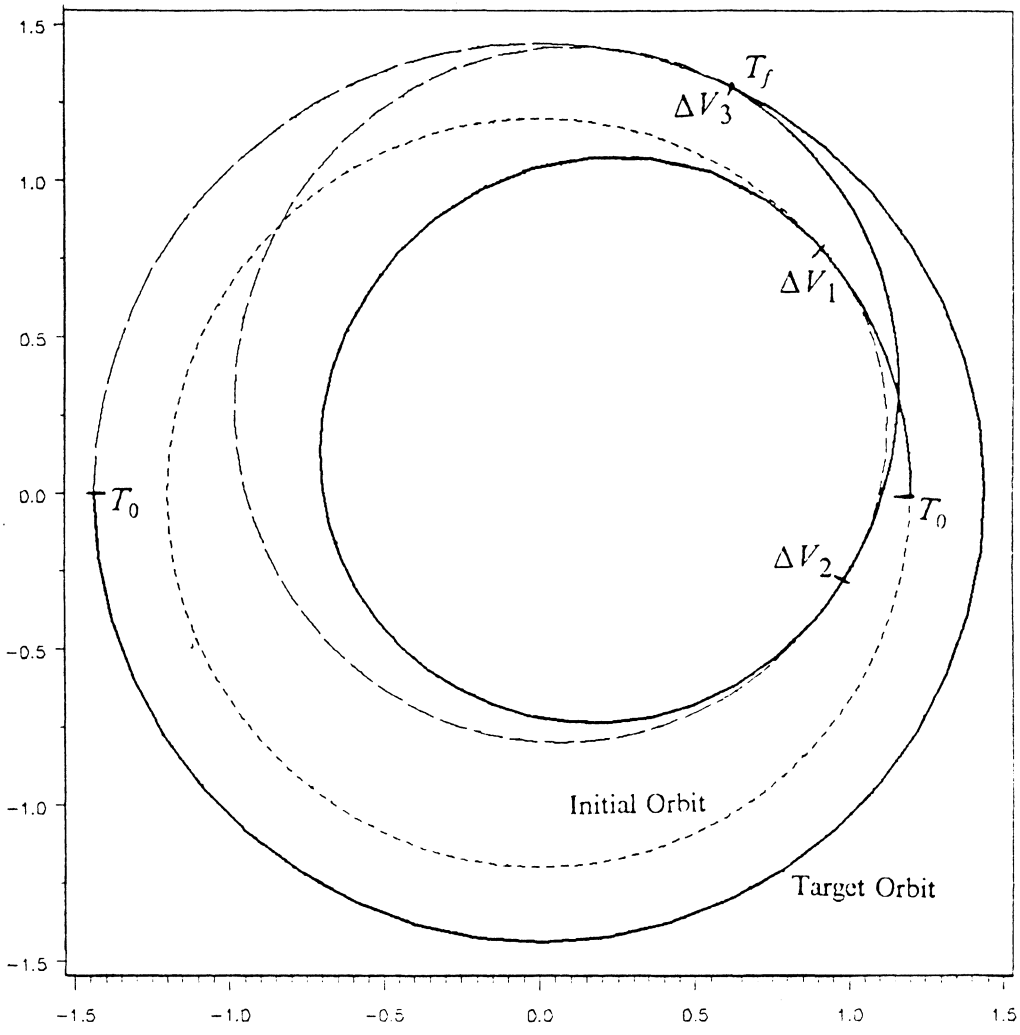

Figure 3. Rendezvous Trajectory between two circles of radius ratio = 1.2 for total time to rendezvous = 7.437 TU.

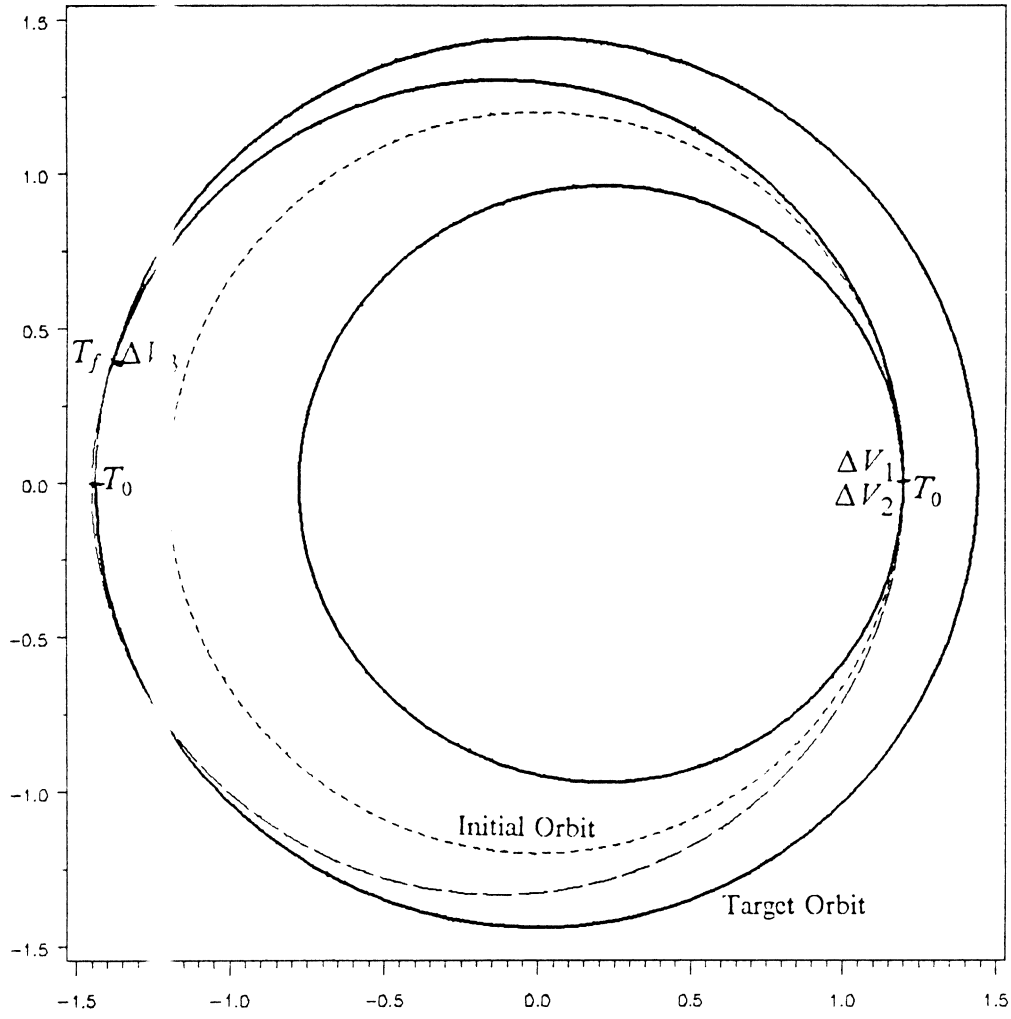

Figure 4. Ren ezvous Trajectory between two circles of radius ratio = 1.2 for t tal time to rendezvous = 10.41 TU.

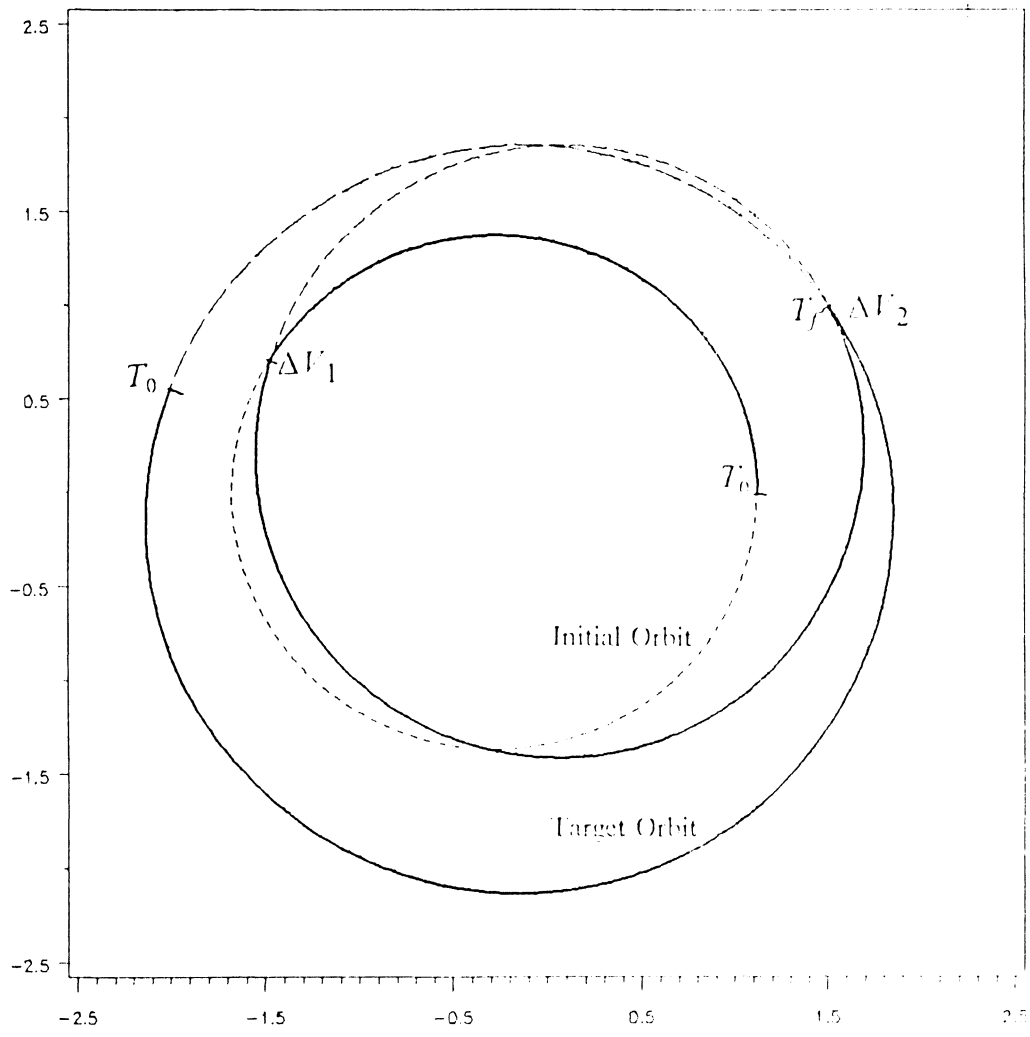

Figure 5. Two-Impulse Time Free Rendezvous Trajectory between two Ellipses of different eccentricity.

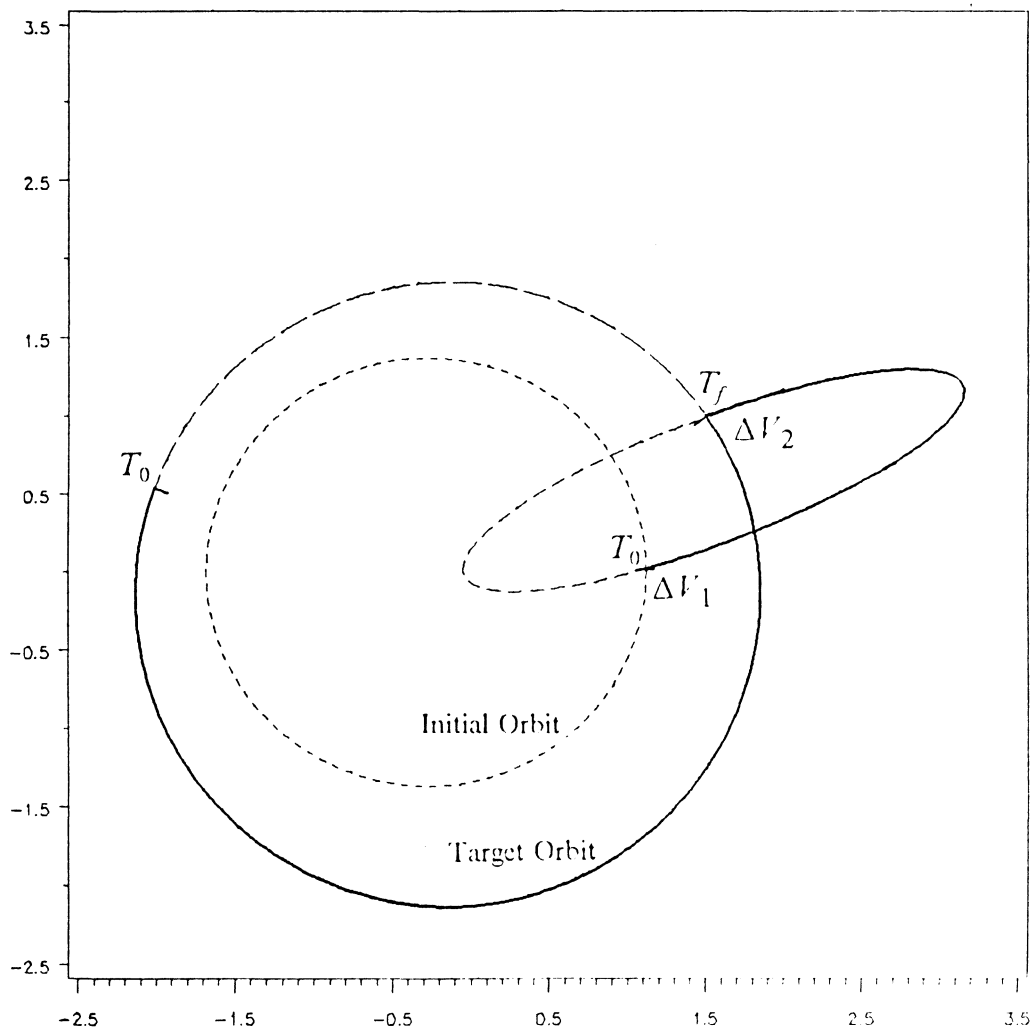

Figure 6. Two-Impulse near rectilinear Time Free Rendezvous Trajectory between two Ellipses of different eccentricity.

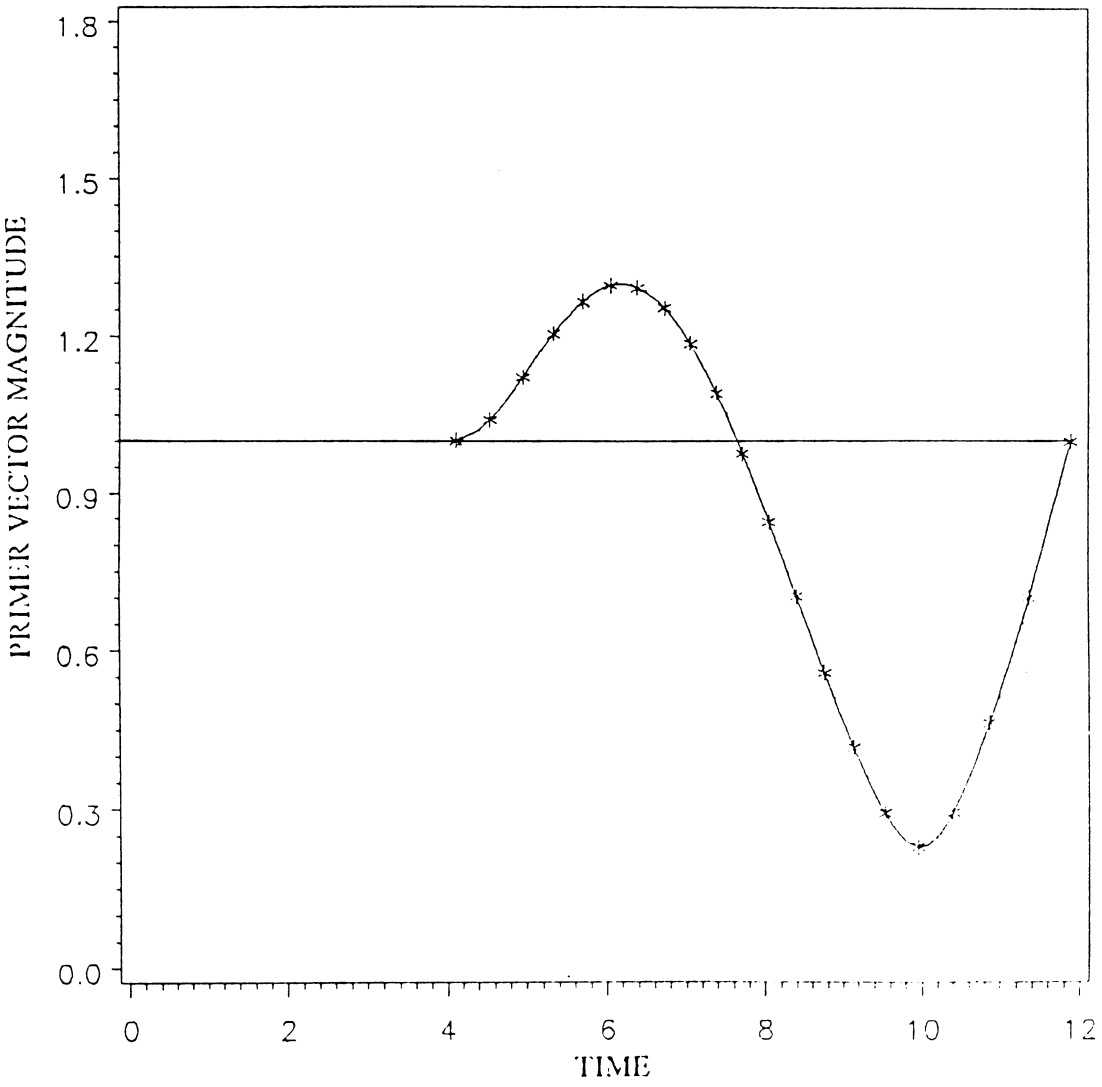

Figure 7. Time history of the Primer-Vector Magnitude of the trajectory corresponding to figure 6.

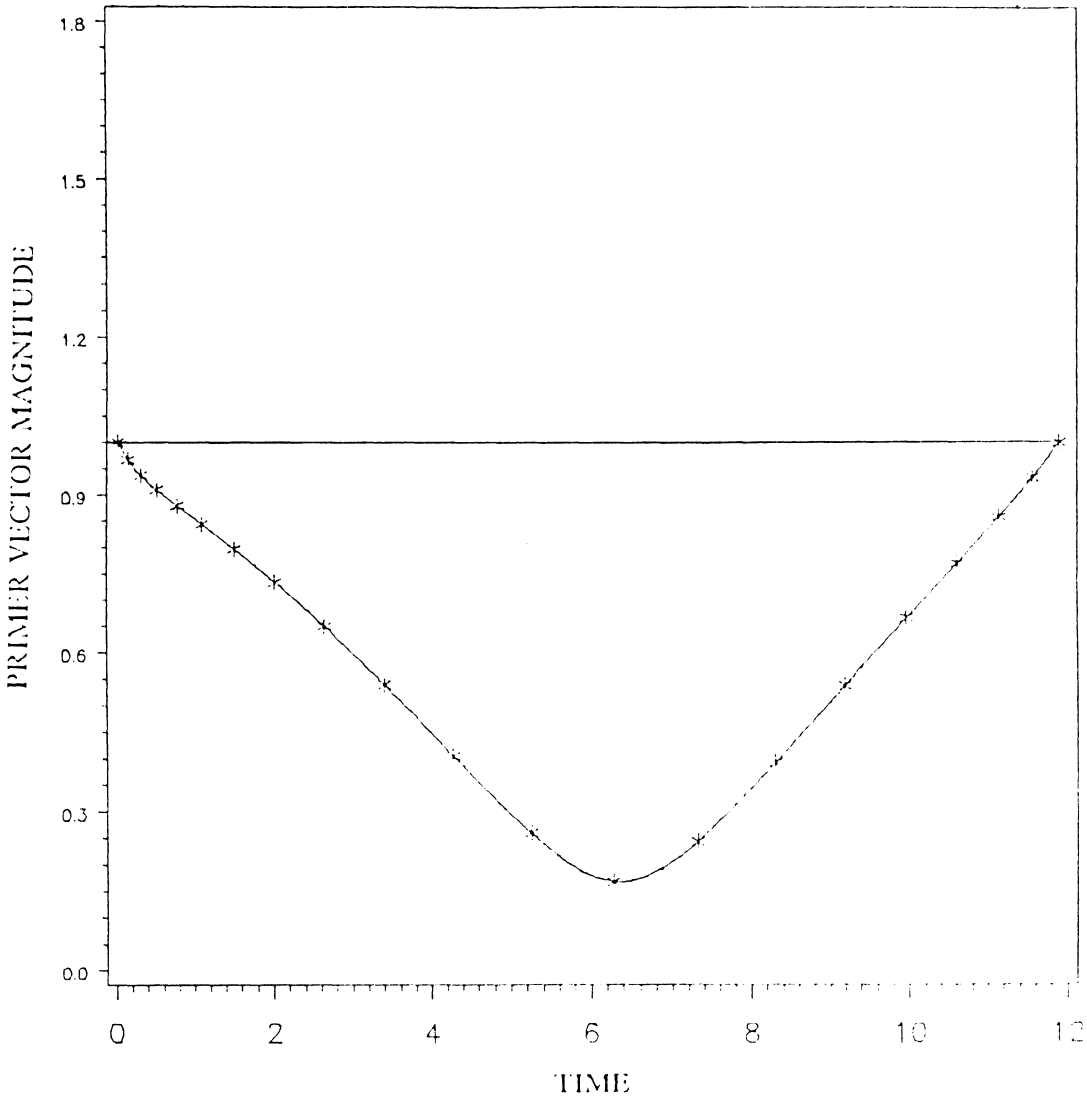

Figure 8. Time history of the Primer-Vector Magnitude of the trajectory corresponding to figure 7.

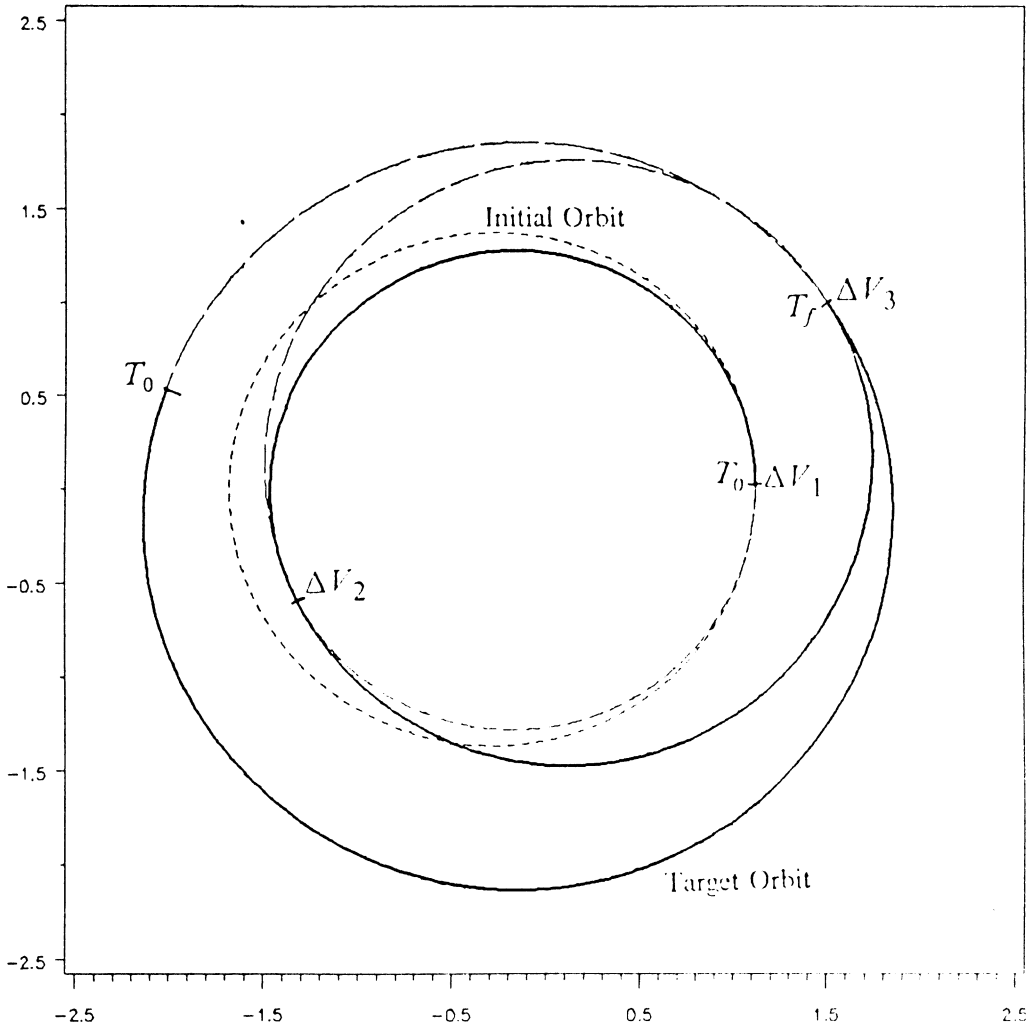

Figure 9. Three-Impulse Time Free Rendezvous Trajectory between two Ellipses of different eccentricity.

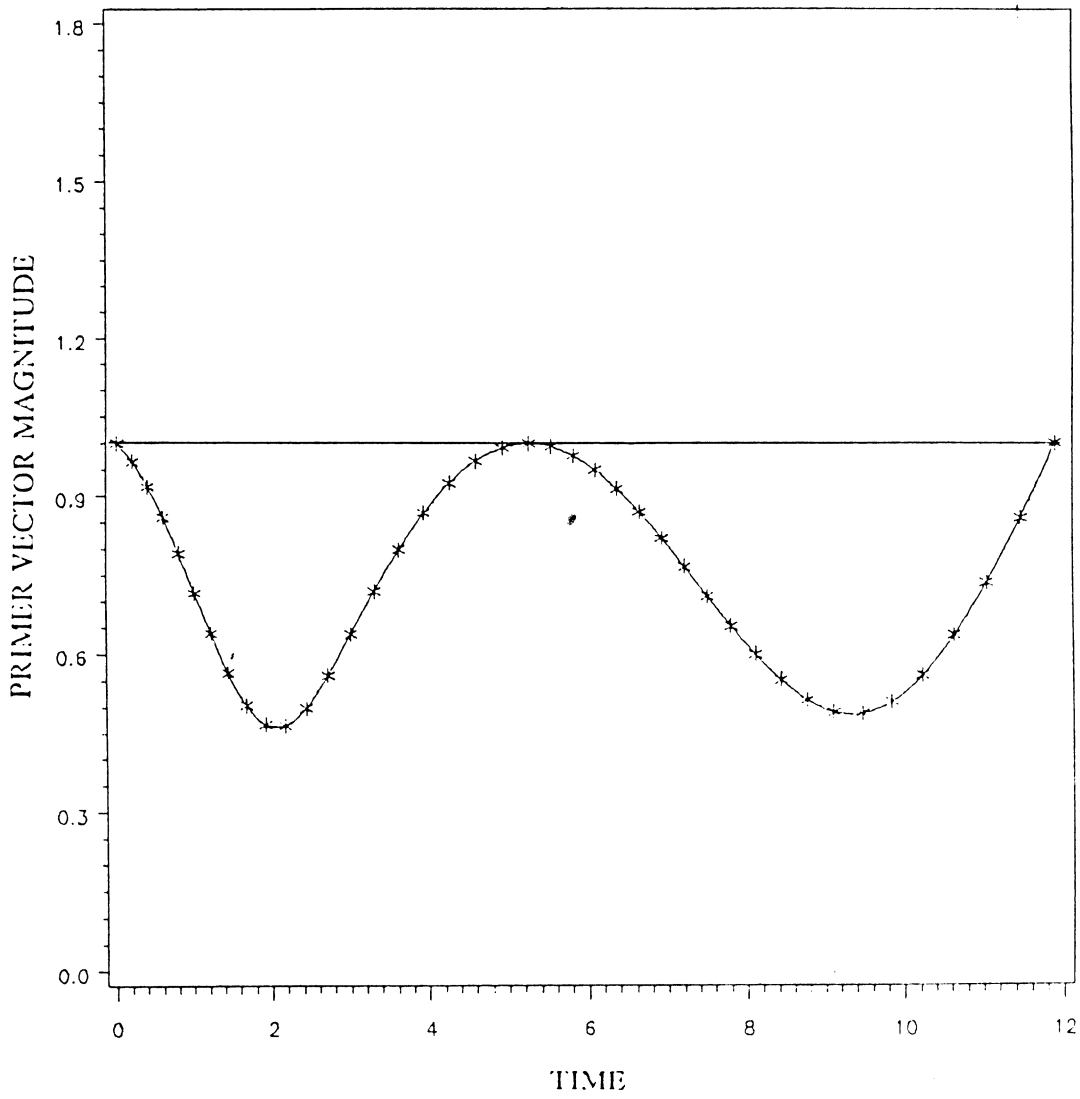

Figure 10. Time history of the Primer-Vector Magnitude of the trajectory corresponding to figure 10.

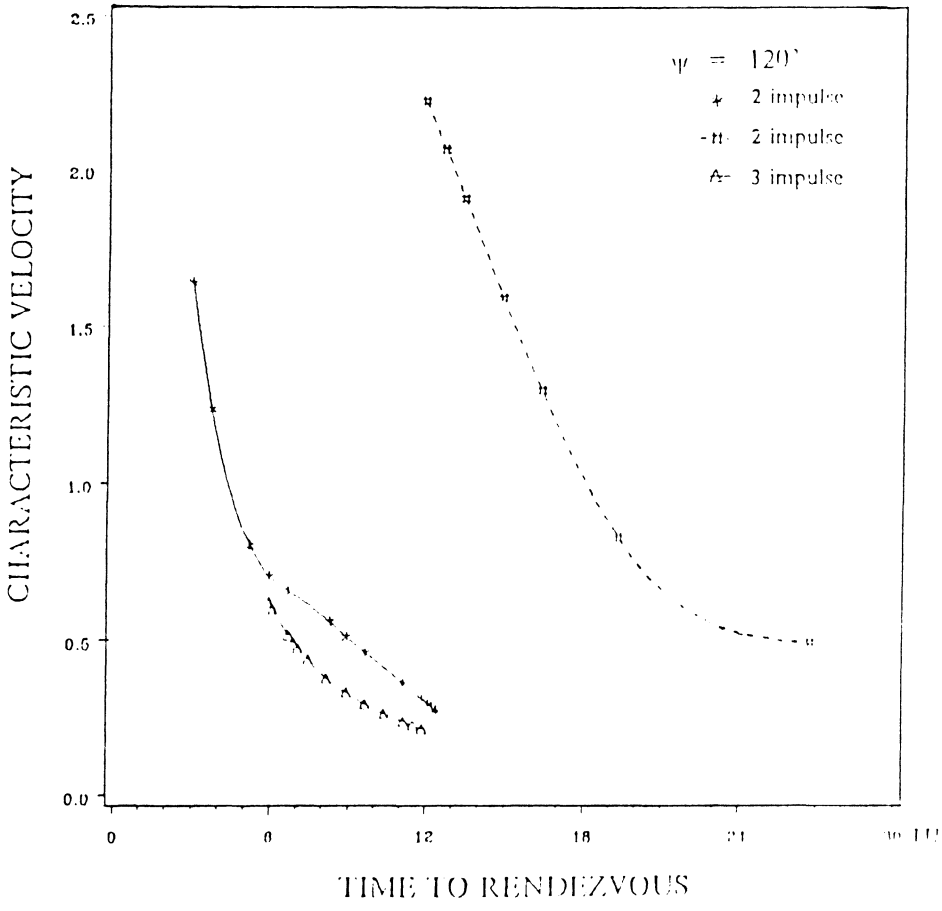

Figure 11. Variation of the Characteristic Velocity with total time for Unconstrained Ellipse-to-Ellipse Rendezvous Problem.

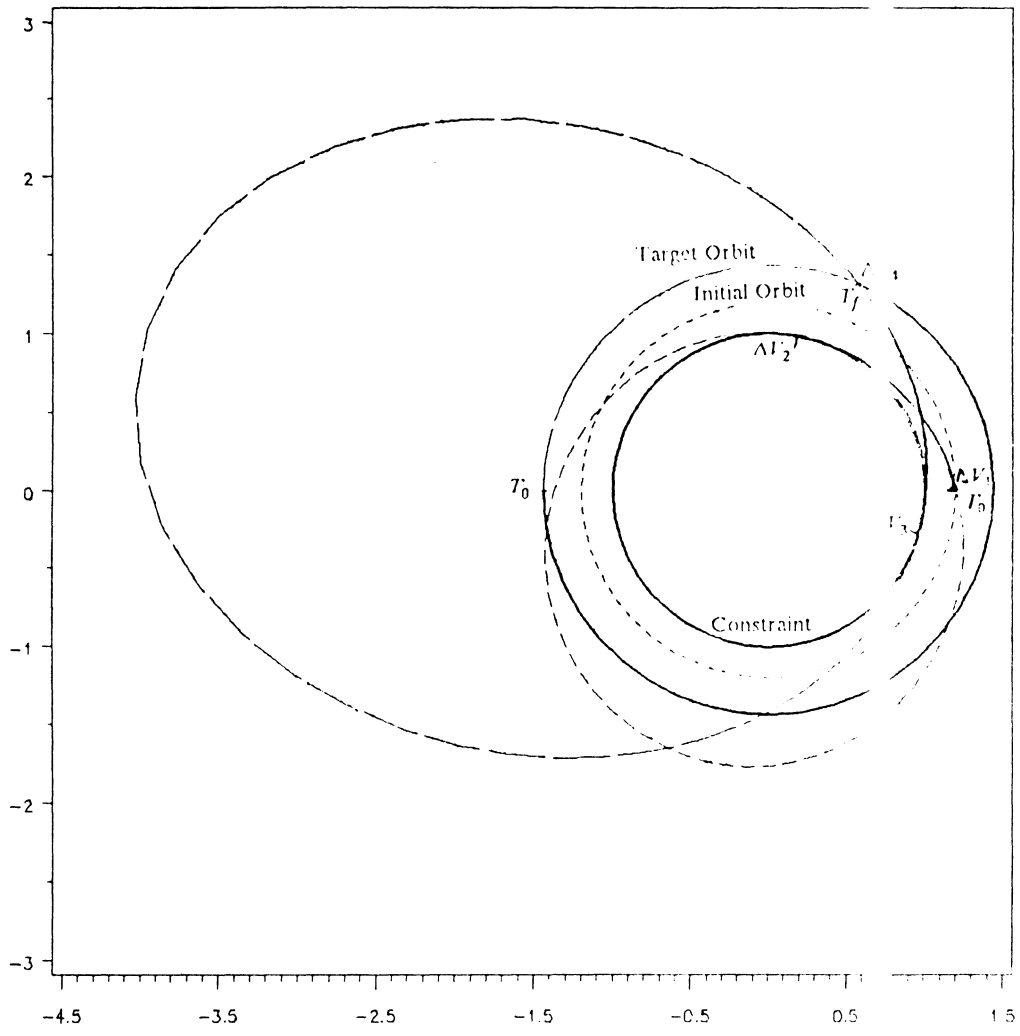

Figure 12. Rendezvous Trajectory between two circles including a Constraint Arc.

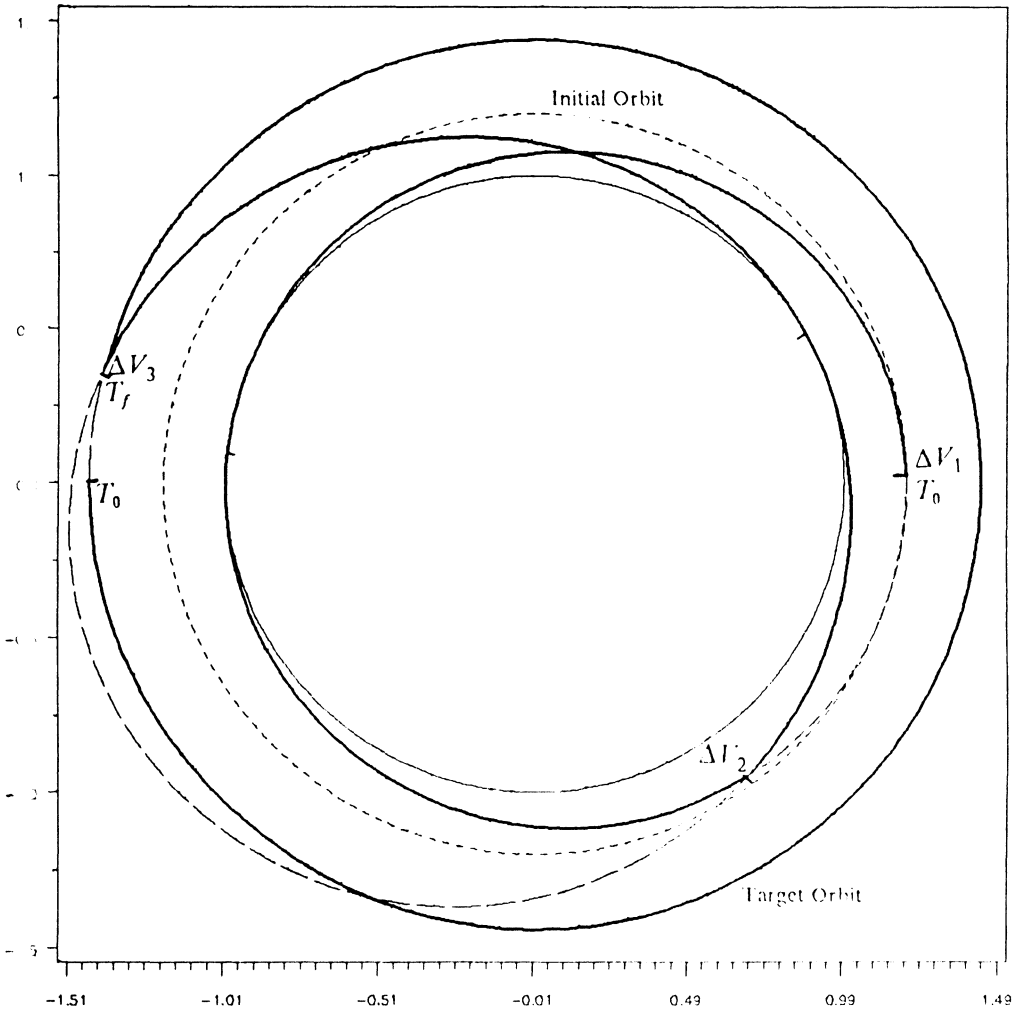

Figure 3. Rendezvous Trajectory between two circles including a Touch-Point.

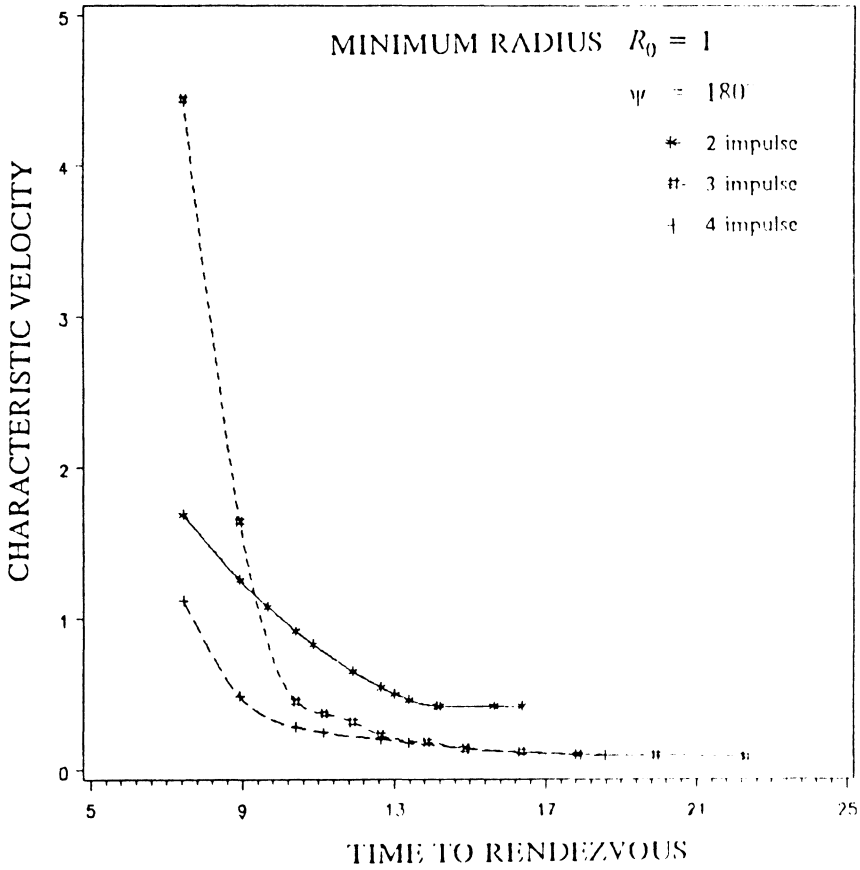

Figure 14. Variation of the Characteristic Velocity with total time for Circle-to-Circle Rendezvous including Minimum Radius Constraint

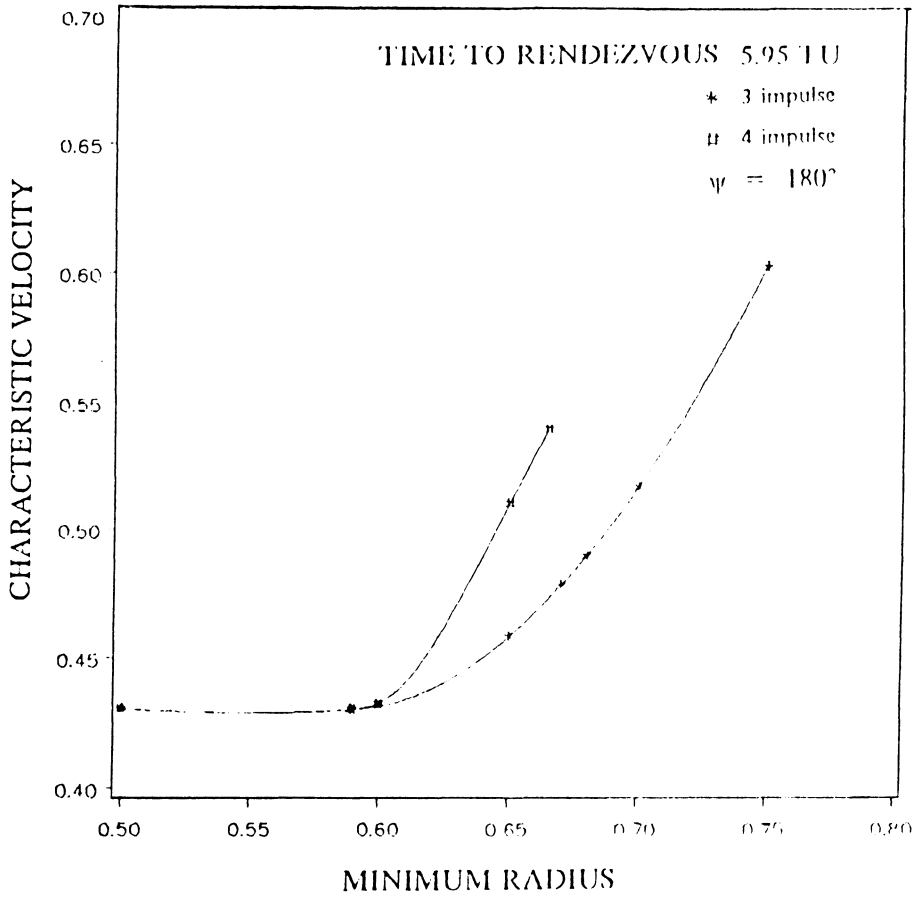

Figure 15. Variation of the Characteristic Velocity with Minimum Radius Constraint.

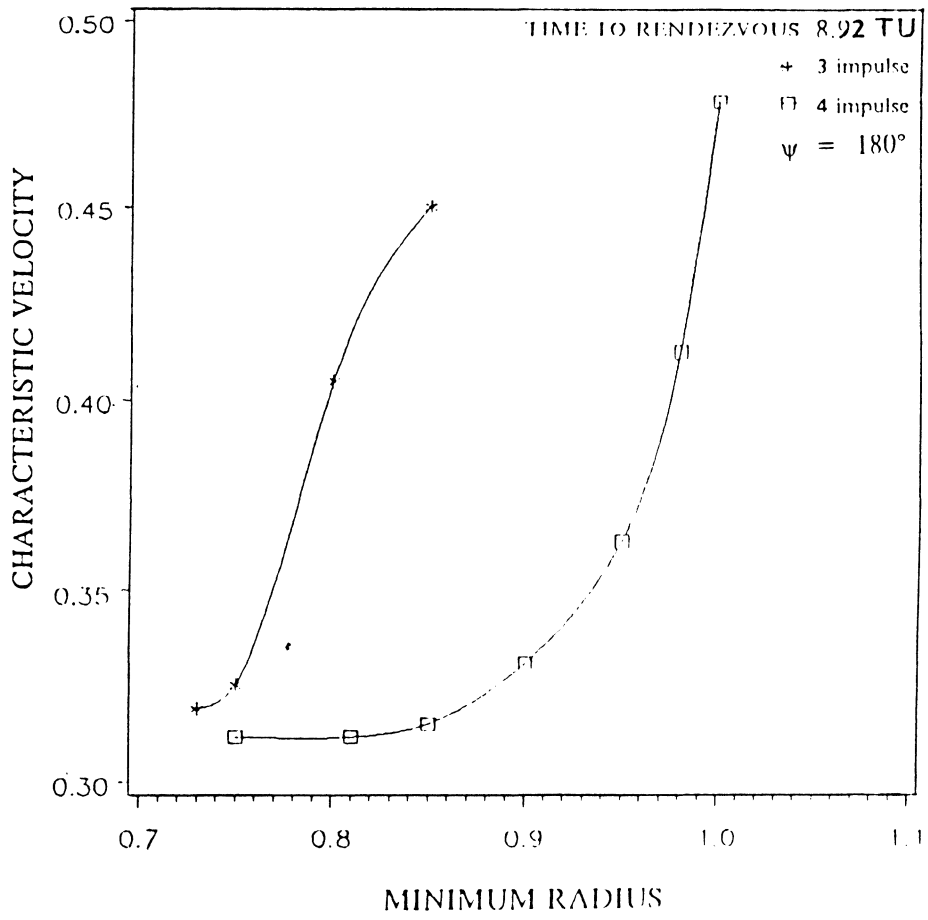

Figure 16. Variation of the Characteristic Velocity with Minimum Radius Constraint.

Appendix A. Solutions to the Costate Equations.

The costate equations for a coasting arc can be written in the state space form as -

$$\begin{Bmatrix} \dot{\lambda}_r \\ \dot{\lambda}_\theta \\ \dot{\lambda}_v \\ \dot{\lambda}_h \end{Bmatrix} = \begin{bmatrix} 0 & \frac{2h}{r^3} & \left(\frac{3h^2}{r^4} - \frac{2}{r^3}\right) & 0 \\ 0 & 0 & 0 & 0 \\ -1 & 0 & 0 & 0 \\ 0 & \frac{-1}{r^2} & \frac{-2h}{r^3} & 0 \end{bmatrix} \begin{Bmatrix} \lambda_r \\ \lambda_\theta \\ \lambda_v \\ \lambda_h \end{Bmatrix} \qquad [A.1]$$

This is a linear system with time-varying coefficients and hence the solution can be written in the form

$$\underset{\sim}{\dot{\lambda}}(t) = \underline{\Phi}(t, t_0)\ \underset{\sim}{\lambda}_0 \qquad [A.2]$$

where $\Phi(t, t_0)$ is the transition matrix. The transition matrix Φ satisfies

$$\dot{\varphi}_{1,i} = \frac{2h}{r^3}\,\varphi_{2,i} + \left\{\frac{3h^2}{r^4} - \frac{2}{r^3}\right\}\,\varphi_{3,i} \qquad [A.3]$$

$$\dot{\varphi}_{2,i} = 0 \qquad [A.4]$$

$$\dot{\varphi}_{3,i} = -\,\varphi_{1,i} \qquad [A.5]$$

$$\dot{\varphi}_{4,i} = -\frac{\varphi_{2,i}}{r^2} - \frac{2h}{r^3}\,\varphi_{3,1} \qquad [A.6]$$

and $\Phi(t_0\,,\ t_0)$ = Identity matrix. Thus

$$\varphi_{2,1} = \varphi_{3,1} = \varphi_{4,1} = 0 \qquad [A.7]$$

and

$$\varphi_{2,2} = 1 \qquad [A.8]$$

Expressions for $\varphi_{3,i}$

Differentiating (A.5) with respect to time and substituting for $\dot{\varphi}_{1,i}$ from (A.3) and expressing $\varphi_{2,i}$ in terms of the Kronecker delta

$$\ddot{\varphi}_{3,i} + \frac{2h}{r^3}\,\delta_{2,i} + \left\{\frac{3h^2}{r^4} - \frac{2}{r^3}\right\}\,\varphi_{3,i} = 0 \qquad [A.9]$$

The above equation can be transformed to the true anomaly derivative using the transformation $\frac{d}{dt}(\ ) = \frac{h}{r^2}\frac{d}{d\theta}(\ )$. Therefore

$$(1 + e \cos\theta)\ \varphi''_{3,i} - 2e \sin\theta\ \varphi'_{3,i} + (1 + 3e \cos\theta)\ \varphi_{3,i} = -2h\,\delta_{2,i} \quad [A.10]$$

Now it can be verified that for $e \neq 0$, $B_i \sin\theta$ is a solution to the homogenous part of (A.10) and $-\frac{\delta_{2,i}\,h}{e} \cos\theta$ is a particular solution. To obtain the other homogenous solution, a variation of parameters type method can be utilized, i.e. assume $f(\theta) = B_i(\theta) \cdot \sin\theta$. A second order ordinary differential equation is then obtained:

$$\left(\sin\theta + \frac{e}{2}\sin 2\theta\right) B'' + 2(\cos\theta + e\cos 2\theta)\ B' = 0$$

On integrating once:

$$B' = \frac{C}{\sin^2\theta\,(1 + e\cos\theta)^2}$$

This can be integrated in three ways depending on the value of e , by transforming to eccentric anomaly E when $e \neq 1$ and to half angles when $e = 1$. Therefore

$$\varphi_{3,i} = -\frac{\delta_{2,i}\,h}{e} \cos\theta + B_i \sin\theta + C_i f(\theta) \quad [A.11]$$

where $f(\theta)$ is given by

for $e < 1$

$$f(\theta) = \frac{-\cos E + 3e - 3e^2\cos E + e^3 - 3e^2 E \sin E + e^3 \sin^2 E}{(1 - e\cos E)\ (1 - e^2)^2} \quad [A.12]$$

for $e = 1$

$$f(0) = \frac{2 - \cos 0 - 4\cos^2 0 - 2\cos^3 0}{5(1 + \cos 0)^2} \qquad [A.13]$$

for $e > 1$

$$f(0) = \frac{-e^3 + 3e^2 \cosh E - 3e + \cosh E - 3e^2 E \sinh E}{(e^2 - 1)^2(e\cosh E - 1)} + \frac{e^3 \sinh^2 E}{(e^2 - 1)^2(e\cosh E - 1)} \qquad [A.14]$$

For $e = 0$ the equation (A.9) becomes

$$\varphi''_{3,i} + \frac{\varphi_{3,i}}{r^3} = -\frac{2h\,\delta_{2,i}}{r^3} \qquad [A.15]$$

which has the solution

$$\varphi_{3,i} = C_i \cos\frac{\theta}{\sqrt{r^3}} + B_i \sin\frac{\theta}{\sqrt{r^3}} - 2h\,\delta_{2,i} \qquad [A.16]$$

Expressions for $\varphi_{1,i}$

Now $\varphi_{1,i} = -\dot{\varphi}_{3,i}$ . . Therefore for $e \neq 0$, $\varphi_{1,i}$ is given by

$$\varphi_{1,i} = \frac{-\delta_{2,i}\, h^2 \sin\theta}{e\, r^2} - \frac{B_i\, h \cos\theta}{r^2} - C_i\, g(\theta) \qquad [A.17]$$

where for $e < 1$

$$g(\theta) = \frac{h}{r^2 \sqrt{(1-e^2)}} \left\{ \frac{\sin E - 3\, e^2 E \cos E + e^3 \sin 2E}{(1-e^2)^2} + h\, e \sin E\, f(\theta) \right\} \qquad [A.18]$$

for $e = 1$

$$g(\theta) = \frac{h \sin\theta\, (5 + 7\cos\theta + 6\cos^2\theta + 2\cos^3\theta)}{5\, r^2 (1+\cos\theta)^3} \qquad [A.19]$$

for $e > 1$

$$g(\theta) = \frac{h}{r^2 \sqrt{(e^2-1)}} \left\{ \frac{\sinh E - 3\, e^2 E \cosh E + e^3 \sinh 2E}{(e^2-1)^2} + h\, e \sinh E\, f(\theta) \right\} \qquad [A.20]$$

For $e = 0$, $\varphi_{1,i}$ is given by

$$\varphi_{1,i} = -\frac{1}{r^3}\left(- C_i \sin\frac{\theta}{\sqrt{r^3}} + B_i \cos\frac{\theta}{\sqrt{r^3}} \right) \qquad [A.21]$$

Expressions for $\varphi_{4,i}$

Transforming $\varphi_{4,i}$ equation to a derivative with respect to the true anomaly θ:

$$\varphi'_{4,i} = \frac{-\delta_{2,i}}{h} - \frac{2}{r}\left(\frac{-\delta_{2,i}\,h}{e}\cos\theta + B_i \sin\theta + C_i f(\theta)\right) \qquad [A.22]$$

On integrating

$$\varphi_{4,i} = D_i + \frac{2\,\delta_{2,i}}{e\,h}\sin\theta + \frac{\delta_{2,i}\sin 2\theta}{2h} + \frac{2\,B_i}{h^2}\cos\theta + \frac{e\,B_i}{h^2}\cos^2\theta - 2\,C_i\,I \qquad [A.23]$$

where for $e < 1$

$$I = \frac{1}{a(1-e^2)^4}\left[\left(\frac{3e}{2} - 2e^3 + \frac{e^5}{2}\right)\theta - (1-e^2)^2\sin\theta - \frac{e}{4}(1-e^4)\sin 2\theta\right] + \frac{3\,e\,E}{a(1-e^2)^{1.5}(1-e\cos E)^2} - \frac{1}{a(1-e^2)^3}\{(6e - 2e^3)\theta + 6e^2\sin\theta + e^3\sin 2\theta\} \qquad [A.24]$$

for $e = 1$

$$I = \frac{1}{5h^2}\left(\tan\frac{\theta}{2} - 2\sin\theta - \frac{\sin 2\theta}{2}\right) \qquad [A.25]$$

for $e > 1$

$$I = \frac{1}{a(e^2-1)^4}\left[\left(\frac{-3e}{2} + 2e^3 - \frac{e^5}{2}\right)\theta + (e^2-1)^2\sin\theta - \frac{e}{4}(e^4-1)\sin 2\theta\right] + \frac{3\,e\,E}{a(e^2-1)^{1.5}(e\cosh E - 1)^2} - \qquad [A.26]$$

$$\frac{1}{a\,(e^2 - 1)^3}\ \{(6\,e - 2\,e^3)\,\theta + 6\,e^2\,\sin\theta + e^3\,\sin 2\theta\}$$

When $e = 0$ the equation (A.6) can be rewritten as

$$\varphi'_{4\,i} = \frac{-\,\delta_{2\,i}}{h} - \frac{2}{r}\,(C_i\,\cos\frac{\theta}{\sqrt{r^3}} + B_i\,\sin\frac{\theta}{\sqrt{r^3}} - 2\,\delta_{2\,i}\,h) \qquad [A.27]$$

This when integrated yields

$$\varphi_{4\,i} = D_i - \frac{\delta_{2\,i}}{h}\,\theta - \frac{2}{r}\,(C_i\sqrt{r^3}\,\sin\frac{\theta}{\sqrt{r^3}} - B_i\sqrt{r^3}\,\cos\frac{\theta}{\sqrt{r^3}} - 2\,\delta_{2\,i}\,h\,\theta) \qquad [A.28]$$

Appendix B. Notes on Parameter Optimization

The candidate trajectories are generated using a parameter optimization technique. This method uses the Kelley-Speyer variable-metric gradient-projection algorithm described by Lefton and Kelley [1978]. Since then several refinements have been made in the projection algorithm notably due to Kelley, Lefton and Johnson [1978] and Das, Cliff and Kelley [1984]. This algorithm is available as a FORTRAN computer program for solving parameter optimization problems.

This program requires a user supplied subroutine FUN1 to generate the cost function, constraint functions and their partial derivatives with respect to the parameters of the problem. The algorithm operates in two phases - constraint correction phase and a curvilinear optimization search phase. These are repeated alternately until the process has converged or until a preset maximum number of cycles is reached. Details of the convergence criteria are described in Lefton and Kelley [1978].

When the number of parameters exceeded six, a more careful handling of the program was found to be needed. As an initial guess, a set of parameters which approximately satisfies all the constraints need to be supplied. It is advisable to appropriately scale the parameters and the gradients of the cost and constraint functions to the same order of magnitude. The program was also found to be very sensitive to the terminal convergence parameter epsilons - EPS1 and EPS2 and the tolerances on the constraints GBAR. For this study, these were set to $10^{-6}, 10^{-3}$ and 10^{-6} respectively. To obtain four impulse trajectories, these values were relaxed slightly to obtain an initial convergence. This solution was then used as the starting guess for the optimization program for the next level of tolerances. For this problem, it was found that convergence could be enhanced at times by altering the one-dimensional search epsilons EPSO and SPEPS and the starting search step-size RODG.

To verify the necessary conditions for optimality, computation of the costates and the Hamiltonian are required. For multiple impulse trajectories, it was observed that difference in the Hamiltonian across an impulse and the time derivative of the primer vector at the impulse depend greatly on the convergence level of the process. For instance, though the cost function did not vary much when the epsilons EPS1 and EPS2 are set to $10^{-8}, 10^{-4}$ respectively and the GBAR set to 10^{-8}, the difference in the Hamiltonian across an impulse reduced by two orders of magnitude. However, the computational effort required for this much convergence is very high. Therefore, to determine whether or not a trajectory satisfies the necessary conditions, the costate λ_θ should also be

examined. On an optimal trajectory, across an impulse, the difference in this variable is of the same order of magnitude as the difference in the Hamiltonian.

Often to obtain a candidate trajectory using the program, the optimization process abruptly stops indicating a terminal error. If IER = 6, the solution can usually be accepted as a feasible solution. If IER = 9, then by altering the EPS2 value, it could be made to converge. If IER = 1, at least three possibilities are known to exist. Tolerance on GBAR is too small (the constraints are very tight) and the program cannot satisfy all the constraints within the required limits of tolerance. In the second case, the program encounters a corner. The third case is that, the initial guess itself represents the correct solution! In all these cases, the solution can sometimes be made to converge by perturbing the starting solution.

The vita has been removed
from the scanned document